

CRITERIA FOR GUARDRAIL NEED AND
LOCATION ON EMBANKMENTS
VOLUME I: DEVELOPMENT OF CRITERIA

by

Hayes E. Ross, Jr.
Associate Research Engineer

and

Edward R. Post
Assistant Research Engineer

Research Report 140-4
Volume I

Evaluation of the Roadway Environment by
Dynamic Analysis of the Interaction Between
the Vehicle, Passenger, and Roadway

Research Study No. 2-5-69-140

Sponsored by
The Texas Highway Department

in cooperation with the
U. S. Department of Transportation, Federal Highway Administration

April 1972

TEXAS TRANSPORTATION INSTITUTE
Texas A&M University
College Station, Texas

FOREWORD

The information contained herein was developed on Research Project 2-5-69-140 entitled "Evaluation of the Roadside Environment by Dynamic Analysis of the Interaction Between the Vehicle, Passenger, and Roadway" which is a cooperative research study sponsored jointly by the Texas Highway Department and the U. S. Department of Transportation, Federal Highway Administration.

Basically, the objectives of the study are to apply mathematical simulation techniques in determining the dynamic behavior of automobiles and their occupants when in collision with various roadside objects or when traversing curves in the road, shoulders, or other situations. It is a continuing study, having been initiated in September 1968.

As part of the first year's work, the computer program HVOSM (formerly known as CALSVA) was obtained from Cornell Aeronautical Laboratory and made operational on the IBM 360 computer facilities at Texas A&M University. In adapting the program, additions and modifications were made which increased its flexibility and usefulness. These changes and the input requirements of the program are documented in Research Report 140-1.

The primary emphasis of the second year's work was the development of an analytical model which predicts the dynamic response of an automobile's occupant in three-dimensional space. Research Report 140-2 presents the derivation of the occupant model, a validation study, and a description of computer input data for determining the occupant's response.

In the 1970-71 year the emphasis was on application of HVOSM to specific roadway design problems. Research Report 140-3 describes an investigation of the *traffic-safe* characteristics of different sloping culvert grate configurations. Criteria are presented for designing a *traffic-safe* sloping grate.

Volume I of this report describes the development of criteria from which the need and location of guardrail on embankments can be determined. Volume II contains the computer input for all runs made in the study and sample output.

The opinions, findings, and conclusions expressed in this publication are those of the authors and not necessarily those of the Texas Highway Department or the Federal Highway Administration.

ABSTRACT

Key Words: Accidents, Automobile, Ditch, Embankments, Encroachments, Guardrail, Impact, Math Models, Safety.

The Highway-Vehicle-Object Simulation Model (HVOSM), a computer model describing an automobile and capable of predicting the dynamic response of the automobile traversing selected terrain, was used to study the behavior of a standard size automobile traversing embankment side slopes at various speeds and departure angles. The accelerations obtained were used to compute a severity index which was then compared with a similarly computed severity index (from actual crash data) of a vehicle impacting a "W-beam" guardrail with posts on 6'3" spacing. An "Equal Severity Curve" was then developed which can be used as a guardrail installation criteria, determining if guardrail should be used to prevent an automobile from going over a selected embankment slope. The amount of guardrail called for by this criteria is less than that required by a similar guardrail installation criteria of California, based on accident experience, and is substantially less than the guardrail required by criteria in the Texas Highway Department Design Manual. The results can be used for guardrail installation criteria on embankments if the accident parameters of 60 mph and 25 degree departure angle are accepted.

The HVOSM was also used to establish a range of distances away from a traveled lane that guardrail should be installed when such installation is located on a 6:1 side slope.

SUMMARY

Highway engineers have had only meager amounts of information to make an objective decision regarding the need and location of guardrail. In many cases criteria are based on the results of a particular statistical analysis of accident information, compiled by the California Division of Highways in 1966. The results of that study, while of significance for the specific guardrails used in California during the period of the accident records (before 1966), should be used with discretion on other guardrail designs. The guardrail, used in California during this period, was mounted on post spaced either on 10 foot centers or on 12 1/2 foot centers. As the post spacing decreases the lateral stiffness of the guardrail increases. In general, as the lateral stiffness of guardrail increases its resistance to impact deformation increases, and as a consequence the collision severity increases. In Texas, most of the guardrail is supported on posts spaced on 6 foot-3 inch centers. The analysis techniques used in the study reported here were general and permit the consideration of a wide range of guardrail types.

To determine the severity of an automobile traversing an embankment a mathematical simulation was used. The orientation and accelerations of the automobile were computed as it traversed the embankment. A combination of mathematical simulations and full-scale test data was used to determine the severity of an automobile in collision with a guardrail. Accelerations at the center of gravity of the automobile served as the indicator of severity.

Guardrail should be used for conditions where the severity of an errant automobile redirected by the guardrail is less than the severity of the automobile traversing the unprotected embankment. For an automobile leaving the roadway at 60 mph with a 25 degree encroachment angle, criteria are presented for selecting the less severe alternative i.e., guardrail versus no guardrail. The criteria are developed for a steel W-beam guardrail with 6 ft.-3 in. post spacing. This is the primary type guardrail used by the Texas Highway Department. The results indicate that many embankments configuration that require guardrail protection by current criteria do not actually need protection.

In another phase of this study, an investigation was made to determine the relative severity between the W-beam guardrail with 6 ft.-3 in. post spacing and no guardrail for a 3:1 embankment, 20 feet in depth with a flat-bottom ditch, and various automobile encroachment conditions (50 mph, 60 mph, and 70 mph in combination with encroachment angles of 10 degrees, 17.5 degrees, and 25 degrees). It was concluded that for shallow angles, a guardrail collision is slightly higher in severity than traversing the 3:1 embankment. However, the severity of traversing the embankment becomes greater than striking a guardrail at speeds in excess of 55 mph and encroachment angles in excess of approximately 22 degrees.

Highways which traverse irregular terrain often contain sections where considerable fill heights are required. A 6:1 slope extending 20 feet from the shoulder's edge is often provided and the remainder of the fill is a 1 1/2:1 slope. Guardrail protection is needed for the steeper slope and this phase of the study determined a safe lateral

distance for locating the guardrail if it is placed on the 6:1 slope. It was concluded that the rail should be no closer than 12 feet from the shoulder's edge.

IMPLEMENTATION STATEMENT

The primary type of guardrail used by the Texas Highway Department is the steel W-beam with 6 ft.-3 in. post spacing. If adopted, the criteria developed in this study would result in much less of this guardrail for embankment protection than now required by present criteria.

An obvious consequence of using less guardrail would be a reduction in material and maintenance costs to the Texas Highway Department. Although more embankment encroachments could be expected, this study shows that the severity of traversing the embankments would be less than that caused by striking a guardrail. Thus, it is probable that accident costs to the motorist would also be reduced. Computation of cost reductions was not within the scope of this project.

The criteria are presented in graphical form for ease of application. An *Equal-Severity-Curve* is plotted, with side slope as the ordinate and ditch depth (fill height) as the abscissa. If a given combination of side slope and ditch depth falls below the curve, guardrail is not recommended, and vice-versa for combinations above the curve. Discretion would obviously be necessary for those configurations below the curve where obstacles exist along or at the bottom of the side slope. In those cases, guardrail in the immediate vicinity of the hazard would probably be needed.

It should be noted that the safer option (guardrail versus no-guardrail) determined by use of this criteria will not necessarily insure a "safe" situation, i.e., severe injuries may still occur. This approach will, however, provide an objective means of selecting

the safer of two hazardous situations.

Another important result of this study pertains to the lateral placement of guardrail on a side slope. The particular embankment studied had a 6:1 slope extending laterally 20 feet from the shoulder's edge, with the remainder of the fill being a 1 1/2:1 slope. It was concluded that if the rail is located on the 6:1 slope it should be 12 feet or greater (up to the 20 foot limit) from the shoulder's edge. Locating it at this distance will minimize the chances of an errant vehicle vaulting the rail.

TABLE OF CONTENTS

Foreword.	ii
Abstract.	iv
Summary	v
Implementation Statement.	viii
List of Figures	xi
List of Tables.	xii
I. Introduction.	1
II. Establishing Guardrail Need	4
Approach.	4
Embankment Study.	5
Guardrail Study	8
Comparison of Relative Severity	12
Parameter Study of Encroachment Conditions	20
III. Locating Guardrail on an Embankment	29
Approach.	29
Results	34
IV. Conclusions	41
Acknowledgments	42
References.	43
Nomenclature.	45
Appendices	
A. Mathematical Model of an Automobile	46
B. Evaluation Criteria	50
C. Severity-Index.	58

LIST OF FIGURES

FIGURE NO.	TITLE	PAGE
1	EMBANKMENT GEOMETRY AND CG PATH OF AUTOMOBILE	6
2	SEVERITY COMPARISON OF AUTOMOBILE TRAVERSING AN EMBANKMENT VERSUS GUARDRAIL REDIRECTION	14
3	WARRANT FOR GUARDRAIL ON EMBANKMENTS	18
4	COMPARISON OF WARRANTS FOR GUARDRAIL ON EMBANKMENTS	19
5	GUARDRAIL AND EMBANKMENT SEVERITY AS FUNCTION OF ENCROACHMENT SPEED AND ANGLE	27
6	ROADSIDE GEOMETRY, ELEVATION VIEW	31
7	ROADSIDE GEOMETRY, PLAN VIEW	32
8	VEHICLE PATHS	35
9	RIGHT FRONT BUMPER HEIGHT, RUN 1, 60 MPH, 25°	37
10	RIGHT FRONT BUMPER HEIGHT, RUN 2, 60 MPH, 15°	38
11	RIGHT FRONT BUMPER HEIGHT, RUN 3, 60 MPH, 15°	39
12	RIGHT FRONT BUMPER HEIGHT, RUN 4, 60 MPH, 15°	40
A1	IDEALIZATION OF AUTOMOBILE (2,3)	48
B1	HUMAN BODY PEAK ACCELERATION LIMITS FOR VARIOUS RISE TIMES, TIME DURATIONS, AND DIRECTIONS (4)	53
B2	ELLIPSOIDAL ENVELOPE FOR DEFINING THE MULTIAXIAL ACCELERATION LIMITS (4)	54
C1	MEASURED (OR COMPUTED) AND LIMIT ACCELERATION COMPONENTS	60

LIST OF TABLES

TABLE NO.	TITLE	PAGE
1	SIMULATION RESULTS ON EMBANKMENTS OF VARIOUS HEIGHTS AND SLOPES	7
2	GUARDRAIL FULL-SCALE CRASH TESTS BY SwRI (8)	10
3	GUARDRAIL FULL-SCALE CRASH TESTS BY CALIFORNIA (10)	13
4	EQUAL SEVERITY COMBINATIONS	17
5	COMPUTED GUARDRAIL SEVERITY INDICES	24
6	SIMULATION RESULTS ON 20 FOOT/3:1 SLOPE EMBANKMENT	26
7	DETAILS OF COMPUTER RUNS	33
B1	LIMIT ACCELERATIONS (G's)	57

I. INTRODUCTION

When a vehicle, travelling at a high speed, leaves the roadway and strikes a guardrail, a hazardous situation obviously exists. It is also hazardous when there is no guardrail and the vehicle must traverse the ditch. Neither event is desirable. Nevertheless, for a given type of guardrail, a given ditch or embankment configuration, and given vehicle encroachment conditions, one situation will be less severe than the other. The primary objective of this study was to develop criteria from which the less severe condition can be selected.

To determine the need for guardrail on embankments many highway engineers are using criteria developed by Glennon and Tamburri (11). Their study was based on a statistical analysis of accident information from the California state highways during 1963 and 1964. The major limitation of this criteria is that it may only be appropriate for guardrails of the type used in California during the time of the accident records. There were two basic types; a spring-mounted curved metal plate guardrail on 10 ft. post spacing; and a blocked out W-section corrugated beam on 12 ft.-6 in. post spacing.

A W-section corrugated beam on posts spaced at 6 ft.-3 in. is the primary type of guardrail used by the Texas Highway Department. The criteria developed here are based in part on full-scale crash tests of this rail system, with one exception. In all but one of the reported test the rail was blocked out from the post, a feature not used by the Texas Highway Department. It is the writers' opinion however that vehicle accelerations resulting from an impact with the blocked out rail

will be approximately the same as those from an impact with the Texas rail.

The approach of this study parallels that of Glennon and Tamburri (11) in that an *Equal-Severity-Curve* is established for determining the less severe alternative, guardrail or an unprotected embankment. For an errant vehicle, the curve represents the combination of embankment heights and slopes which are equal in severity to impacting a particular guardrail. The major difference of the two approaches is the basis for measuring accident (guardrail impacts and embankment traversals) severity. In the referenced work, weighted severity values were assigned to different occupant injury levels as determined from the accident reports. The study used a combination of math models and full-scale test data to determine vehicle accelerations during guardrail impacts and embankment traversals. Vehicle accelerations served as the measure of severity.

In establishing need criteria, math models provide more flexibility than accident records. This method is not limited to studying a particular type of guardrail and any conceivable embankment configuration can be investigated. Also, the problem of interpreting accident reports does not exist.

In terrain where large fill heights are required, a 6:1 slope is often provided up to 20 feet off the shoulder's edge and a 1 1/2:1 slope from that point to the bottom of the fill. Guardrail protection is usually provided for the steeper 1 1/2:1 slope. The final phase of this study was addressed to the question: If the rail is placed on the 6:1

slope, how far off the shoulder should it be located to minimize the possibility of an automobile vaulting it?

II. ESTABLISHING GUARDRAIL NEED

Approach

A mathematical model of an automobile, described in Appendix A, was used to determine the orientation and accelerations of an automobile as it traverses an embankment. A mathematical model (9) and full-scale test data (7, 8, 10, 13) were used to determine the accelerations of an automobile impacting a guardrail. Accelerations at the center of gravity of the automobile were used as the measure of severity. A severity index, discussed in Appendices B and C, served to quantify the relative severity of each event for an unrestrained occupant.

To compare the severity of a vehicle impacting a guardrail with the severity of a vehicle traversing an embankment one should use the same vehicle under the same encroachment conditions. These requirements were maintained as closely as possible. In the mathematical model studies of embankment encroachments, a 1963 Ford Galaxie was used, as discussed in Appendix A. In most of the cases analyzed, a vehicle of similar size was used in the full-scale guardrail tests. For vehicle encroachment conditions, a 25 degree angle of departure and a speed of 60 mph were selected. These encroachment conditions are the criteria recommended for the structural design of guardrails (16).

A parameter study was made to evaluate the effects of encroachment conditions on the severity of an embankment traversal and a guardrail collision. The embankment in each case was a 3:1 side slope, 20 feet in height, with a flat-bottom ditch.

Embankment Study

The basic geometry of each embankment investigated consisted of a 10-foot shoulder adjoining a side slope of $b:a$ and height H , with a flat bottom ditch, as shown in Figure 1. Slopes ($b:a$) of 2:1, 3:1, and 6:1 in combination with heights (H) of 10 feet, 20 feet, 30 feet, and 50 feet were studied. In addition, a 3.25:1 slope with a height of 20 feet and a 4:1 slope with a height of 20 feet were studied. The reason for studying the latter two cases is explained in the section entitled "Comparison of Relative Severity".

In the 14 embankment combinations studied, the simulated automobile was placed on the roadway with an initial velocity and encroachment angle, θ_1 . Throughout the maneuvers, the automobile was assumed to be out of control, that is, no attempt was made to steer the automobile.

A summary of the 14 runs and the results are shown in Table 1. Reference is made to Figure A1 of Appendix A for the roll, pitch, and yaw axes of the automobile.

In most cases, as can be seen in Table 1, the encroachment angle and speed of the automobile increases as the vehicle traverses the embankment slope. In all but the 6:1 slope combinations the automobile became completely airborne (all tires off ground) for a period of time after leaving the shoulder. In traversing a 2:1 slope with a height of 10 feet, the automobile landed on the ditch bottom and then pitched over about its front end. For all other height and slope combinations, the automobile landed on the embankment slope after being airborne with no tendency to roll or pitch over.

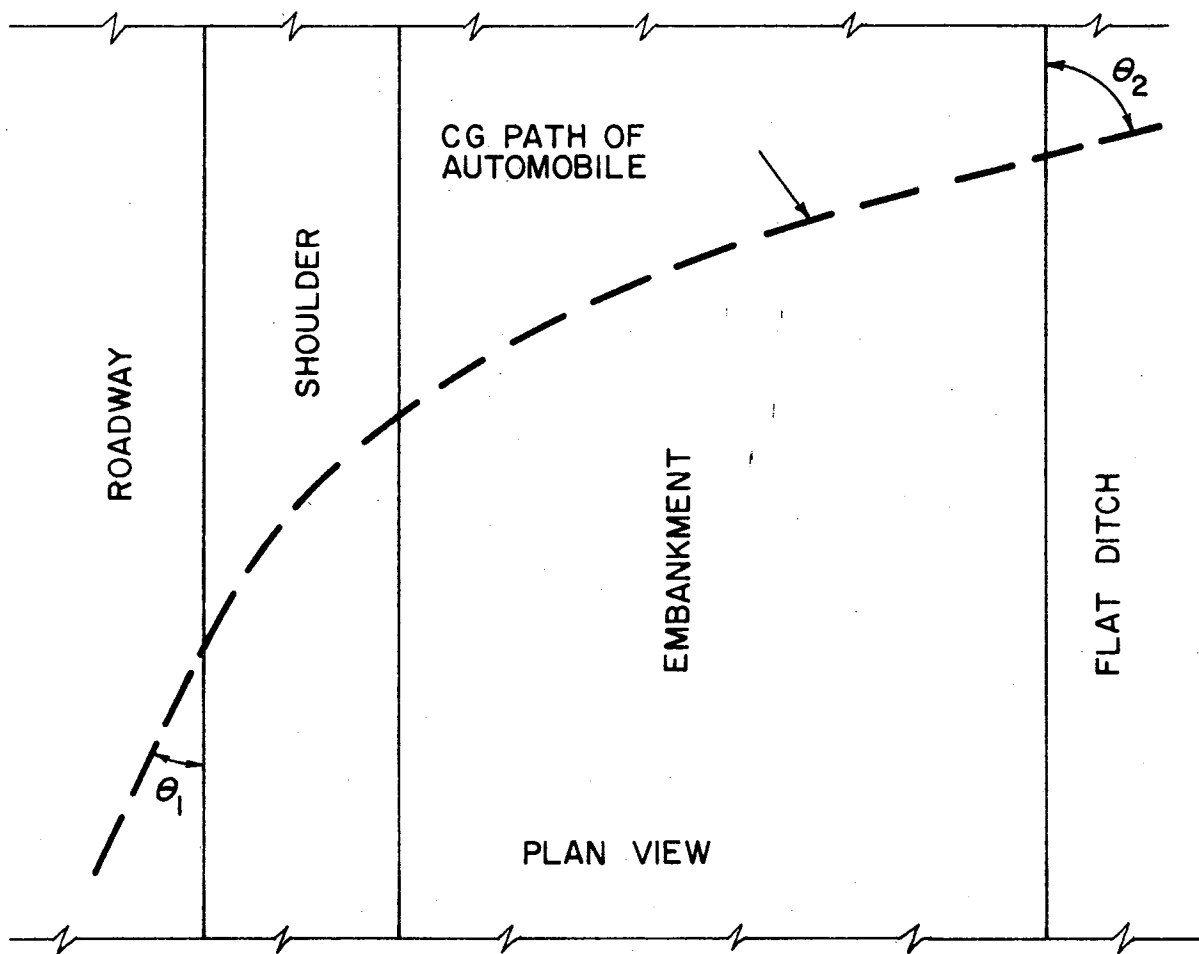
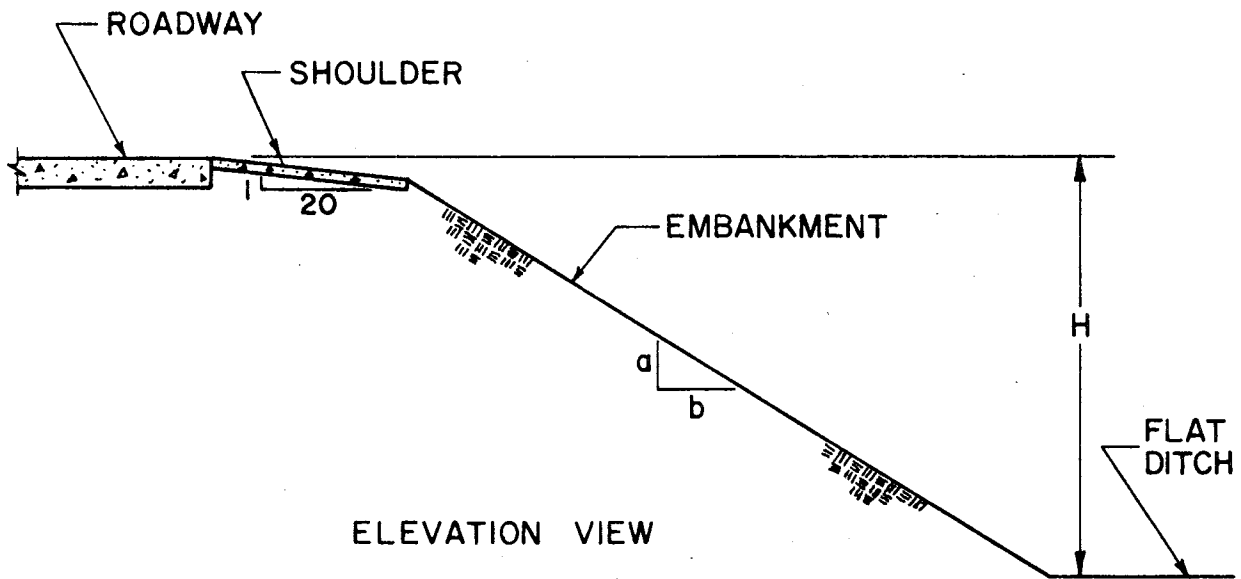


FIGURE 1. EMBANKMENT GEOMETRY AND CG PATH OF AUTOMOBILE

TABLE 1

SIMULATION RESULTS ON EMBANKMENTS OF VARIOUS HEIGHTS AND SLOPES

ENCROACHMENT SPEED = 60 MPH SHOULDER WIDTH = 10 FT.
 ENCROACHMENT ANGLE (θ_1) = 25 DEG SHOULDER SLOPE = 20:1

RUN NUMBER	TERRAIN		AUTOMOBILE							
	EMBANKMENT HEIGHT (H) (FT)	EMBANKMENT SLOPE (b:a)	MAXIMUM ROLL ANGLE (DEG)	MAXIMUM PITCH ANGLE (DEG)	ANGLE (DEG) AUTOMOBILE CONTACTS FLAT DITCH (θ_2)	SPEED (MPH) AUTOMOBILE CONTACTS FLAT DITCH	AVERAGE DECELERATIONS OVER 50 MILLISECONDS			
							$G_{LONG.}$	$G_{LAT.}$	$G_{VERT.}$	SEVERITY INDEX (EQ. B1)
1	10	2:1	33	RO ^a	24	60	2.6	3.4	4.7	1.1 ^b
2	10	3:1	29	10	25	61	0.2	0.6	5.3	0.9
3	10	6:1	11	5	29	62	0.1	0.3	2.2	0.4
4	20	2:1	48	15	24	62	2.6	4.9	6.3	1.5
5	20	3:1	30	12	40	62	1.3	0.8	7.6	1.3
6	20	6:1	11	5	34	65	0.1	0.4	2.8	0.5
7	20	3.25:1	27	10	37	64	1.3	0.7	4.5	0.8
8	20	4:1	20	9	30	64	---	0.5	3.7	0.6
9	30	2:1	47	23	32	58	0.3	1.3	6.8	1.2
10	30	3:1	29	13	36	66	0.4	0.9	4.9	0.8
11	30	6:1	11	5	33	67	0.0	0.6	3.5	0.6
12	50	2:1	47	26	66	55	7.6	3.4	9.7	2.1
13	50	3:1	29	13	43	68	1.2	1.3	6.4	1.1
14	50	6:1	11	6	43	70	0.2	0.5	3.7	0.6

a. Automobile rolled over about its front-end as it contacts flat ditch after being airborne

b. Severity-Index when contact with flat ditch occurs (just prior to roll-over)

Also shown in Table 1 are the maximum average decelerations for a 50-millisecond period. These values were obtained by studying the computer output for those times when the larger decelerations occurred and then, by trial and error, selecting the 50-millisecond period with the highest average deceleration. The severity-index was computed from Equation B1 of Appendix B and data from Table B1.

Guardrail Study

The types of guardrail which can be studied by TTI's version of HVOSM are limited to those whose lateral resistance to vehicle penetration is independent of the longitudinal position of the vehicle contact point. Since the W-section guardrail on 6 ft.-3 in. post spacing does not fall in this category, the model could not be applied.

Two independent methods were used to investigate the severity of a guardrail collision. The first method was based on accelerometer information measured in full-scale crash tests by Michie (8) of Southwest Research Institute (SwRI). The second method was based on results obtained by mathematical equations presented by Olson (9). These two independent methods provided results that were in reasonable agreement with each other.

A review of the literature revealed that no full-scale tests have ever been performed on the guardrail system now used in Texas for embankment protection. However, a series of full-scale crash tests (8, 10) have been conducted on a guardrail system similar to the Texas guardrail. The one difference between the two guardrail systems was that the as-tested

rail was blocked-out from the post whereas the Texas rail butts against the post. It is the writer's opinion that the lateral stiffness of the blocked-out system is not significantly different from that of the Texas system, and as a consequence the redirection forces and acceleration on an impacting vehicle will be essentially the same.

The severity-index of guardrail collisions conducted by SwRI (8) were computed and are presented in Table 2. These tests were selected on the basis of being conducted at an impact speed and angle of approximately 60 mph and 25 degrees. Also, the vehicles used in these tests were similar in size and weight to the one used in the simulation studies. The severity-index was computed for longitudinal and lateral decelerations occurring over two time intervals; 50 milliseconds and 325 to 450 milliseconds. The longer time interval was measured from the instant of impact to the time when the automobile becomes parallel to the center line of the guardrail. The severity-index was computed over the longer interval so that it could be compared with the work of Olson (9), which is presented later. As discussed in Appendix B, the tolerable deceleration limits in Table B1 for the two time intervals were based on an interpretation of the findings of Hyde (4). Referring to Table 2, a reasonable comparison exists between four of the six severity-indices measured over the two different time durations.

An analysis of three full-scale crash tests conducted by Beaton (10) at impact conditions of approximately 60 mph and 25 degrees are presented in Table 3. The automobile decelerations perpendicular (G_{LAT}^*)

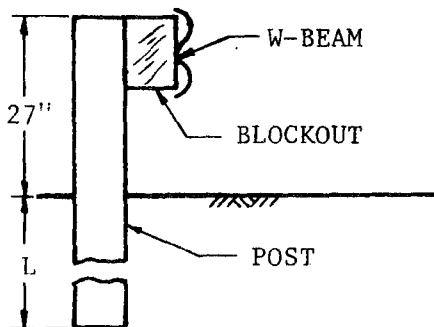


TABLE 2

GUARDRAIL FULL-SCALE CRASH TESTS BY SwRI (8)

RAIL HEIGHT = 27 IN.
POST SPACING = 6 FT.-3 IN.

SwRI TEST NUMBER	GUARDRAIL					AUTOMOBILE								
	TYPE RAIL MEMBER	TYPE POST	BLOCKOUT	POST EMBEDMENT, L (IN.)	DYNAMIC DISPLACEMENT (FT.)	WEIGHT (LBS)	IMPACT SPEED (MPH)	IMPACT ANGLE (DEG)	DECELERATIONS (G's)					
									50 M.S.			325-450 M.S.		
									G _{LONG.}	G _{LAT.}	SEVERITY INDEX ^{a.}	G _{LONG.}	G _{LAT.}	SEVERITY INDEX ^{b.} (EQ. B1)
101	STEEL W-BEAM	8x8 IN. WOOD	8 IN. WOOD	36	4.25	4042	55	31	4.6	4.5	1.1	2.9	3.1	0.9
103	STEEL W-BEAM	8x8 IN. WOOD	8 IN. WOOD	36	2.84	4123	60	22	3.1	6.1	1.3	2.2	3.3	0.9
119	STEEL W-BEAM	6B8.5	NONE	42	2.74	4169	53	30	4.5	4.4	1.1	2.3	2.7	0.8
120	STEEL W-BEAM	6B8.5	1-6B8.5	42	4.05	3813	57	28	3.9	6.6	1.4	2.9	3.5	1.0
121	STEEL W-BEAM	6B8.5	2-6B8.5	42	3.10	4478	56	27	3.6	6.7	1.5	1.9	3.3	0.9
122	STEEL W-BEAM	6B8.5	2-6B8.5	42	4.95	4570	63	25	3.9	7.6	1.6	2.3	3.9	1.0

TOLERABLE ACCELERATION LIMITS (SEE APPENDIX B FOR DISCUSSION)

a. $G_{XL} = 7$ and $G_{YL} = 5$

b. $G_{XL} = 6$ and $G_{YL} = 4$

and parallel (G_{LONG}^*) to the guardrail were computed from the following equations developed by Olson (9), since no acceleration-time data was reported by Beaton.

$$G_{LAT}^* = \frac{V_I^2 \sin^2(\theta)}{2g \{AL \sin(\theta) - B [1 - \cos(\theta)] + D\}} \quad (1)$$

$$G_{LONG}^* = \mu G_{LAT}^* \quad (2)$$

where:

V_I = impact velocity;

θ = impact angle;

AL = distance from front bumper to center of gravity;

2B = width of vehicle; (B = one-half of vehicle width);

D = lateral dynamic displacement of barrier; and

μ = coefficient of friction between vehicle and barrier. A value of 0.3 was used, which is an average value of tests reported in Table A1 of NCHRP Report 86 (9).

The primary assumption in developing these equations was that the deceleration was constant from impact to that time in which the automobile becomes parallel to the guardrail. Olson (9) demonstrated that these equations were accurate within ± 20 percent.

To compute a severity-index, the decelerations computed by Equations 1 and 2 must be transformed to the decelerations along the automobile coordinate system axes as defined in Figure A1 of Appendix A. This was accomplished with the following two transformation equations:

$$G_{L\text{AT.}} = G_{L\text{AT.}}^* [\cos(\theta) - \mu\sin(\theta)] \quad (3)$$

$$G_{L\text{ONG.}} = G_{L\text{AT.}}^* [\sin(\theta) + \mu\cos(\theta)] \quad (4)$$

Observations of high-speed photography show that for the time interval between impact and maximum guardrail displacement (dynamic displacement), the heading angle of the automobile changes only slightly. It is during this interval that the maximum deceleration usually occurs. Therefore, in the above transformation equations, the initial impact angle was used.

A comparison of the severity-indices computed for the California tests in Table 3 with those in Table 2 further demonstrate that the mathematical equations presented by Olson (9) provide reasonable results. Equations 1 through 4 will, therefore, be used later to predict the severity of guardrail collisions for various impact speeds and angles.

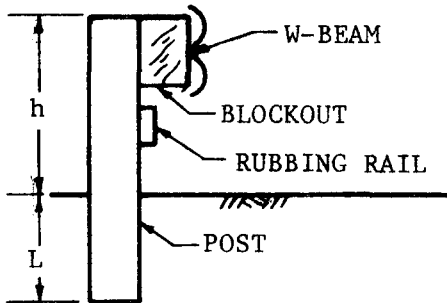
Comparison of Relative Severity

The severity-indices of embankment traversals, from Table 1, are shown plotted in Figure 2. Superimposed on the figure is the range of severity-indices for impacts with the guardrail from Tables 2 and 3. The range of severity-indices shown on Figure 2 for guardrail are based on accelerations averaged over the longer time duration.

It was anticipated that the severity-index would increase as the embankment height increased for a given slope. However, this was not always the case, as the plots in Figure 2 show. Two good examples of

TABLE 3

GUARDRAIL FULL-SCALE CRASH TESTS BY CALIFORNIA (10)



13

CALIF. TEST NUMBER	GUARDRAIL							AUTOMOBILE							
	RAIL MEMBER	POST with 6[8.2 RUBBING RAIL	WOOD POST BLOCKOUT (IN)	POST SPACING (IN)	POST EMBEDMENT, L (IN)	RAIL HEIGHT, h (IN)	DYNAMIC DISPLACEMENT ¹ (FT)	WEIGHT (LBS)	IMPACT SPEED (MPH)	IMPACT ANGLE (DEG)	AVERAGE DECELERATIONS OVER 275 to 300 M.S.				
											G* LAT. (EQ. 1)	G* LONG. (EQ. 2)	G LAT. (EQ. 3)	G LONG. (EQ. 4)	SEVERITY INDEX (EQ. B1)
106	STEEL W-BEAM	8x8 IN. WOOD	8	6-3	41	30	2.45	4570	60	25	3.9	1.2	3.1	2.7	0.9
107	STEEL W-BEAM	8x8 IN. WOOD	8	6-3	35	27	2.10	4570	60	25	4.2	1.3	3.3	2.9	1.0
108	STEEL W-BEAM	8x8 IN. WOOD	8	6-3	35	24	2.10	4570	59	25	4.1	1.2	3.2	2.8	0.9

1. DYNAMIC DISPLACEMENT TAKEN AS 1.4 TIMES PERMANENT SET [BASED ON RESULTS OF SwRI (8) TESTS ON CALIFORNIA GUARDRAIL SYSTEM]

AUTOMOBILE CHARACTERISTICS

AL = 7.95 FT

2B = 6.5 FT

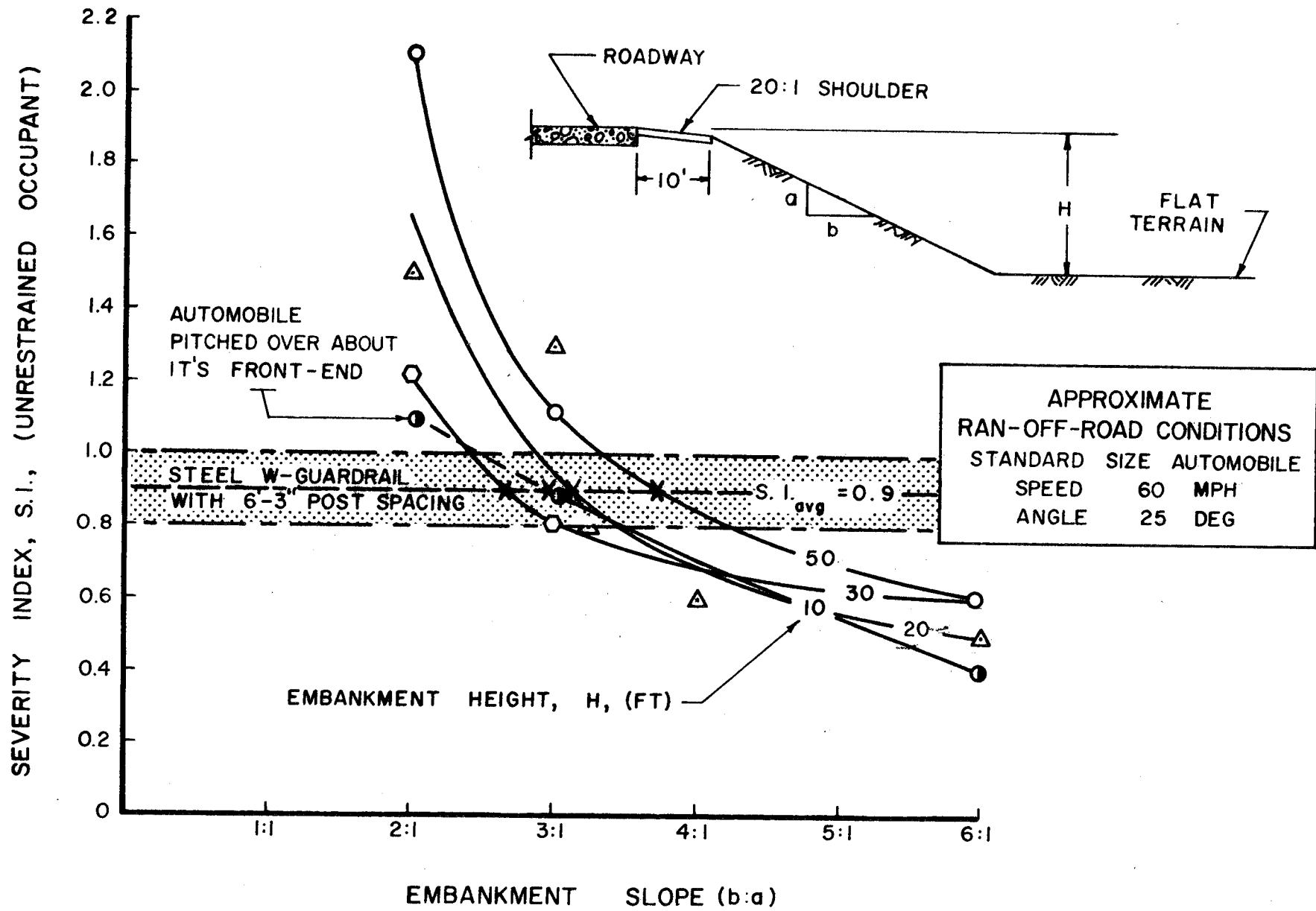


FIGURE 2. SEVERITY COMPARISON OF AUTOMOBILE TRAVERSING AN EMPAKMENT VERSUS GUARDRAIL REDIRECTION

this anomaly are the severity-index for a 2:1 slope with a 20-foot fill height, and for a 3:1 slope with a 20-foot fill height (runs 4 and 5 of Table 1). Both values are considerably higher than anticipated. Examination of the output from runs 4 and 5 showed that when the vehicle reached the flat ditch bottom, both the front and rear bumpers of the automobile simultaneously contacted and penetrated the terrain, causing large resistive forces. In other runs, front and rear bumper contact did not occur simultaneously, and hence, the effect of bumper contact on the severity-index was not as pronounced.

Additional runs (numbered 7 and 8 in Table 1) were made on a 20-foot embankment to determine the variation of the severity-index between a 3:1 and a 6:1 slope because of the large difference in the index between these slopes. As seen in Figure 2, flattening the slope from a 3:1 to a 3.25:1 and to a 4:1 resulted in a considerable reduction in the severity-index. A sharp transition in the severity-index exists at a slope of about 3:1 for the 20-foot embankment height. As mentioned earlier, both front and rear bumper contact occurred simultaneously for the 3:1 slope, and as a consequence, the forces and accelerations were greatly increased. Front and rear bumper contact did not occur simultaneously for the 3.25:1 and the 4:1 slope.

Vehicle attitude during initial contact with the ditch is therefore a major factor influencing the relative severity of an embankment traversal. If in HVOSM, an automobile other than the 1963 Ford had been used, the vehicle's attitude and behavior may have been different, and the relative severities may have differed. The problem of

vehicle selection is not peculiar to simulation studies only but also plagues full-scale test studies. In any case, the results obtained through use of the '63 Ford provide much better data than has been available regarding the severity of embankment traversals.

Table 4 contains those combinations of embankment slope (measured as a ratio and in degrees) and height which are equal in severity to the upper bound, average, and lower bound guardrail severities. Each combination represents the intersection point of a given embankment height curve with a given guardrail severity line in Figure 2. For example, traversal of an embankment with a 3.14:1 (or 18 degree) slope, 20 feet in height, is equal in severity to an automobile impacting the guardrail, based on the "average" guardrail severity.

Equal-Severity-Curves based on the upper and lower bound of guardrail severities are shown in Figure 3. The coordinates of the four points from which each curve was drawn were taken from Table 4.

As shown in Figure 3, a line through a slope equal to 3:1 appears to be an average *Equal-Severity-Curve*. Therefore, an embankment with a slope steeper than a 3:1 should be protected and, conversely, slopes flatter than 3:1 do not need guardrail protection.

Embankment heights less than 10 feet were not investigated and the data must be extrapolated for these heights. Nevertheless, it seems reasonable to assume that a 3:1 slope can also be used as the *Equal-Severity-Curve* for heights up to 10 feet. Implementation of the criteria would be simplified in so doing.

For comparison with this study, other *Equal-Severity-Curves* are shown in Figure 4. The relationship established by Glennon and Tamburri

TABLE 4
EQUAL SEVERITY COMBINATIONS

EMBANKMENT HEIGHT (H) Ft.	EMBANKMENT SLOPE AT INTERSECTION OF GUARDRAIL AND EMBANKMENT SEVERITY-INDEX CURVES*					
	UPPER BOUND (SI = 1.0)		AVERAGE (SI = 0.9)		LOWER BOUND (SI = 0.8)	
	b:a	Deg	b:a	Deg	b:a	Deg
10	2.42:1	22	2.92:1	19	3.50:1	16
20	2.88:1	19	3.14:1	18	3.44:1	16
30	2.42:1	22	2.65:1	21	3.02:1	18
50	3.34:1	17	3.75:1	15	4.26:1	13

* Values obtained from Figure 2

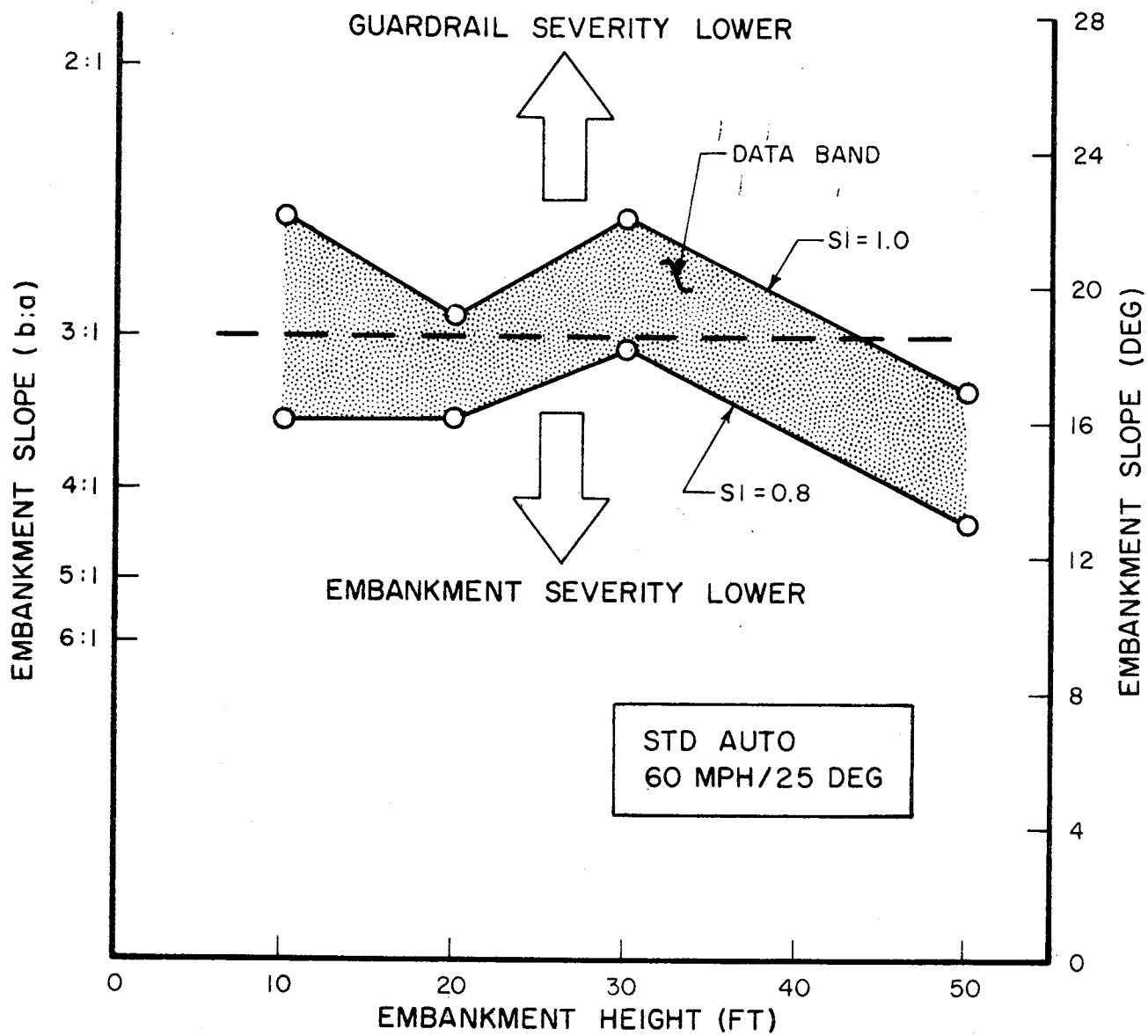


FIGURE 3. WARRANT FOR GUARDRAIL ON EMBANKMENTS

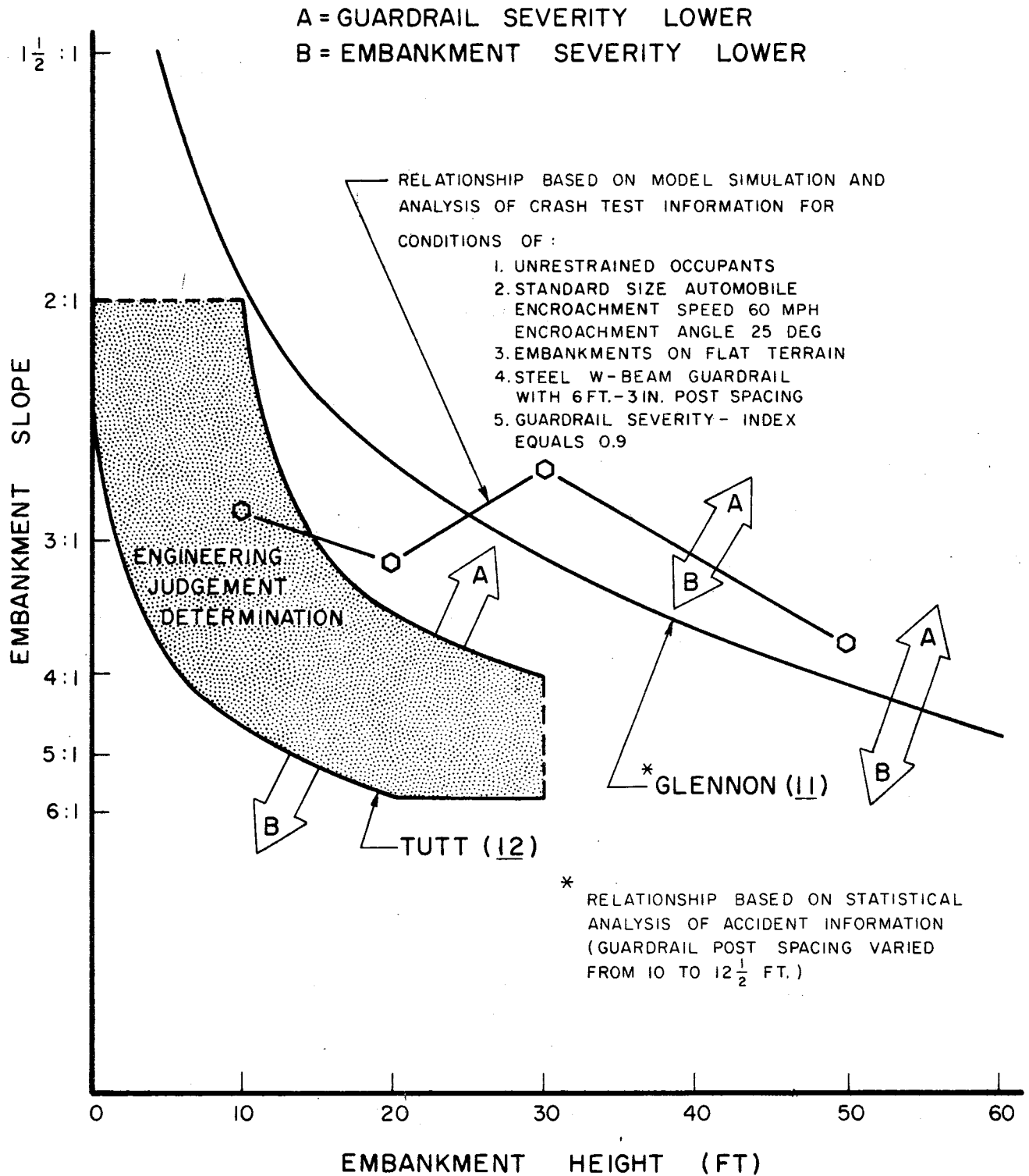


FIGURE 4. COMPARISON OF WARRANTS FOR GUARDRAIL ON EMBANKMENTS

(11) was based on an statistical analysis of accident information compiled on the California highways during the years of 1963 and 1964. Their work is currently used by many highway engineers.

As evident in Figure 4, the relationship established by Glennon and Tamburri generally agrees with the relationship established in this study. The differences existing between these two independently established curves are attributed to the following: (a) the conditions of encroachment of 60 mph and 25 degrees investigated in this study are probably more severe than those conditions occurring in the majority of the accidents statistically analyzed, and (b) the Texas guardrail system is stiffer than that used at the time of the accidents, because of a smaller post spacing.

A guide to determine if guardrail is needed on roadway embankments was also presented by Tutt (12) and is shown on Figure 4. As in the criteria presented by Tutt, engineering judgment will obviously be necessary in applying the results of this study. Where a hazardous condition exists along or at the bottom of the embankment, guardrail may be warranted in the immediate vicinity of the hazard.

Parameter Study of Encroachment Conditions

In previous sections the severity of an automobile traversing different embankment heights and slopes and automobiles in collision with guardrails were presented. The encroachment conditions were 60 mph and a 25-degree approach. To determine what effects the encroachment conditions have on the vehicle's behavior and the severity of the event,

a series of runs were made where the speed and encroachment angle were varied. An embankment having a 3:1 slope and a 20-foot height was selected for the study.

The majority of full-scale crash tests on guardrail have been conducted at an impact speed of 60 mph and angle of 25 degrees. To predict the severity of guardrail for different conditions of impact, the mathematical equations developed by Olson (9) were used. These equations, which were numbered Equations 1 and 2, were shown earlier to compare favorably with measured accelerometer information.

Before Equation 1 could be used, a method was needed to estimate the dynamic displacements, D, of a guardrail for various conditions of impact. This was done by assuming that the displacement of a guardrail is proportional to the kinetic energy expended by an automobile as it is being redirected. The kinetic energy, KE, expended by a guardrail from the instant of impact to that time when the automobile is parallel to the guardrail was approximated as follows:

$$KE = C \left[\frac{1}{2} \frac{W}{g} V_I^2 \sin^2 (\theta) \right] \quad (5)$$

where all terms except C have been described previously. Note that $V_I \sin \theta$ is the component of vehicle velocity which is normal to the guardrail.

Equation 5 neglects the kinetic energy expended by changes in the vertical and longitudinal velocity components. The "C" coefficient is the portion of the kinetic energy of the vehicle expended by the guardrail. The remainder of the energy of impact is expended primarily in sheet metal crushing of the automobile.

Using information from full-scale crash tests, the dynamic displacement of a guardrail was approximated as follows:

$$\left\{ \frac{D}{C \left[\frac{1}{2} \frac{W}{g} V_I^2 \sin^2(\theta) \right]} \right\}_{\text{TEST}} = \left\{ \frac{D}{C \left[\frac{1}{2} \frac{W}{g} V_I^2 \sin^2(\theta) \right]} \right\}_{\text{SELECTED CONDITIONS}}$$

Therefore, assuming $C_{\text{TEST}} = C_{\text{SELECTED CONDITIONS}}$,

$$\left\{ D \right\}_{\text{SELECTED CONDITIONS}} = \left\{ \frac{D}{W V_I^2 \sin^2(\theta)} \right\}_{\text{TEST}} \left\{ W V_I^2 \sin^2(\theta) \right\}_{\text{SELECTED CONDITIONS}}$$

(6)

The values used for the TEST parameters in Equation (6) were selected from the tests on the California guardrail system (8 X 8 in. wood posts), as presented in Table 3. The test values used were:

$$W = 4570 \text{ lbs.},$$

$$D = 2.37 \text{ ft. (average of 4 tests),}$$

$$V_I = 60 \text{ mph} = 88 \text{ fps.},$$

$$\theta = 25 \text{ degrees, and}$$

$$\sin(25) = 0.423.$$

Thus

$$\begin{aligned} \left\{ \frac{D}{W V_I^2 \sin^2(\theta)} \right\}_{\text{TEST}} &= \left\{ \frac{2.37}{(4570)(88)^2(0.423)^2} \right\} \\ &= 3.74 \times 10^{-7} \frac{\text{sec}^2}{\text{LB-FT}} \end{aligned}$$

Equation 6 thus reduced to

$$\left\{ D \right\}_{\text{SELECTED CONDITIONS}} = 3.74 \times 10^{-7} \left\{ W V_I^2 \sin^2 \theta \right\}_{\text{SELECTED CONDITIONS}} \quad (7)$$

The properties of the automobile simulated in HVOSM (1963 Ford Galaxie), which are needed in Equations 1 through 4 and Equation 7, were as follows:

$$W = 4,750 \text{ lbs.},$$

$$AL = 81.52 \text{ in.},$$

$$B = 39.50 \text{ in.}, \text{ and}$$

$$\mu = 0.3$$

Substitution of the above value of W into Equation 7 gives

$$\left\{ D \right\}_{\text{SELECTED CONDITIONS}} = 1.78 \times 10^{-3} \left\{ V_I^2 \sin^2 \theta \right\}_{\text{SELECTED CONDITIONS}} \quad (8)$$

In Table 5, values of V_I and θ listed in columns one and two were inserted in Equation 8 to compute the displacements listed in column three.

To estimate the duration, ΔT , of the guardrail impact, Equation 9 was used.

$$\Delta T = \frac{V_I \sin \theta}{g G_{LAT}^*} \quad (9)$$

The numerator and the denominator of the right hand side of Equation 9 are, respectively, the component of vehicle velocity and the component of vehicle acceleration, both in a direction normal to the guardrail.

The computed decelerations and severity-indices for an automobile redirected by a guardrail for various encroachment conditions are tabulated in Table 5. The tolerable accelerations used to compute the severity-indices are those for the 225-450 millisecond duration, for

TABLE 5

COMPUTED GUARDRAIL SEVERITY INDICES

IMPACT SPEED (V_I) (MPH)	IMPACT ANGLE (θ) (DEG.)	GUARDRAIL DYNAMIC DISPLACEMENT (EQ. 8) (FT.)	G^*_{LAT} (EQ. 1)	G^*_{LONG} (EQ. 2) ($\mu = 0.3$)	TIME DURATION (EQ. 9) (MS)	G_{LONG} (EQ. 3)	G_{LAT} (EQ. 4)	SEVERITY INDEX (EQ. B1)
50	10.0	0.29	1.8	0.5	224	0.8	1.7	0.4
50	17.5	0.86	2.8	0.8	249	1.6	2.4	0.7
50	25.0	1.71	3.5	1.1	276	2.1	2.7	0.8
60	10.0	0.41	2.4	0.7	202	1.1	2.2	0.6
60	17.5	1.25	3.5	1.0	237	2.0	3.0	0.8
60	25.0	2.47	4.3	1.3	271	3.0	3.3	1.0
70	10.0	0.57	2.9	0.9	191	1.4	2.7	0.7
70	17.5	1.70	4.1	1.2	233	2.4	3.6	1.0
70	25.0	3.35	4.9	1.5	273	3.4	3.9	1.1

an unrestrained occupant, given in Table B1.

Table 6 contains the results of the parameter study on the selected embankment (3:1 sideslope, 20 feet in height). The dynamic behavior of an automobile at speeds of 50 mph, 60 mph, and 70 mph and encroachment angles of 10 degrees, 17.5 degrees, and 25 degrees was investigated by HVOSM.

Severity-index curves for guardrail and the typical embankment as a function of encroachment conditions are plotted in Figure 5. The severity curve for the 25-degree embankment traversal shows a sharp decrease as the speed of the automobile increased from 60 mph to 70 mph. Intuitively, this phenomenon appears incorrect. However, as discussed in a previous section, at 60 mph the front and rear bumper of the automobile contacted the ditch bottom simultaneously, causing high resistive forces and accelerations. At 70 mph, front and rear bumper contact did not occur simultaneously and the resistive forces were lower.

For comparative purposes, the severity-index for a 3.25:1 slope and encroachment conditions of 60 mph and 25 degrees (run 7 in Table 1) is shown in Figure 5. If the 3.25:1 slope had been used in the parameter study, it appears that a sharp decrease in the severity index between 60 mph and 70 mph would not have occurred. This phenomenon prompts the following comments:

- (1) For a given vehicle and encroachment conditions, slight changes in embankment conditions can cause large changes in the severity index. As a consequence, discretion should be exercised in extrapolating results to other embankment conditions.

TABLE 6

SIMULATION RESULTS ON 20 FOOT/3:1 SLOPE EMBANKMENT

SHOULDER WIDTH = 10 FT.

SHOULDER SLOPE = 20:1

TERRAIN			AUTOMOBILE									
RUN NUMBER	EMBANKMENT HEIGHT (H) (FT)	EMBANKMENT SLOPE (b:a)	ENCROACHMENT SPEED (MPH)	ENCROACHMENT ANGLE (θ_1) (DEG)	MAXIMUM ROLL ANGLE (DEG)	MAXIMUM PITCH ANGLE (DEG)	ANGLE (DEG) AUTOMOBILE CONTACTS FLAT DITCH (θ_2)	SPEED (MPH) AUTOMOBILE CONTACTS FLAT DITCH	AVERAGE DECELERATIONS OVER 50 MILLISECONDS			
									$G_{LONG.}$	$G_{LAT.}$	$G_{VERT.}$	SEVERITY INDEX (EQ. B1)
15	20	3:1	50	10.0	22	8	26	55	0.6	0.5	2.2	0.4
16	20	3:1	50	17.5	25	10	29	55	0.8	0.8	2.2	0.4
17	20	3:1	50	25.0	27	12	35	54	1.3	0.8	2.9	0.5
18	20	3:1	60	10.0	23	7	23	64	0.6	0.5	2.6	0.5
19	20	3:1	60	17.5	27	9	26	64	0.9	1.0	2.4	0.5
5	20	3:1	60	25.0	30	12	40	62	1.3	0.8	7.6	1.3
20	20	3:1	70	10.0	25	6	19	74	0.5	0.6	2.2	0.4
21	20	3:1	70	17.5	31	9	26	73	1.2	1.1	3.5	0.7
22	20	3:1	70	25.0	32	16	37	69	0.1	1.5	6.1	1.1

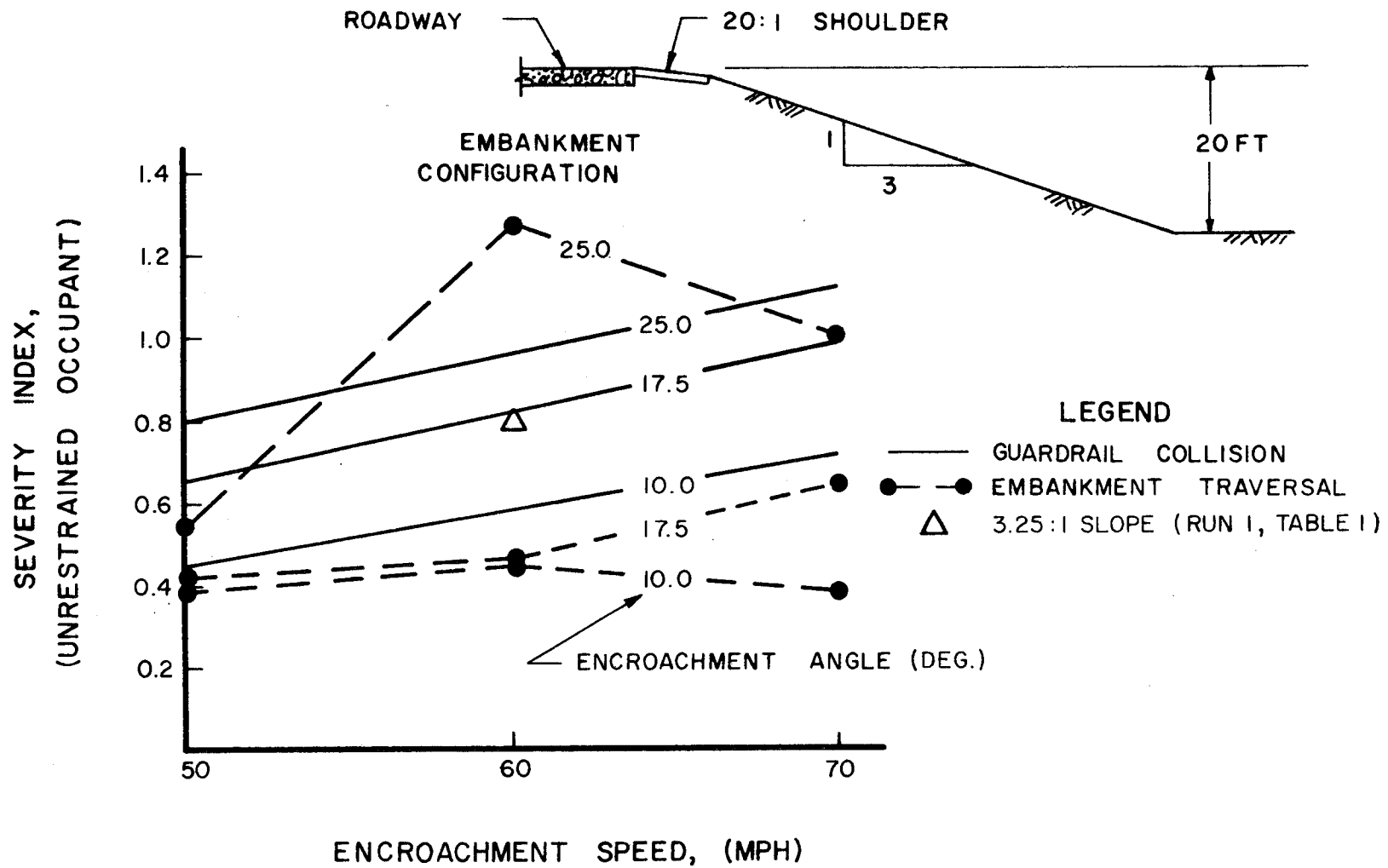


FIGURE 5. GUARDRAIL AND EMBANKMENT SEVERITY AS FUNCTION OF ENCROACHMENT SPEED AND ANGLE

(2) For given embankment conditions and given encroachment conditions, the severity index may vary for different vehicles. However, from a size and weight standpoint, the 1963 Ford used in the simulation studies is representative of a large population of automobiles now in use. The results produced in this study are therefore believed to be applicable to the "mean" automobile population.

For a 17.5-degree angle of encroachment the embankment severity is considerably less than the guardrail severity at all speeds. Consequently, if the roadway conditions are such that the 25-degree encroachment angle is not attainable it may be desirable to develop new criteria based on the reduced encroachment angle. If 17.5 degrees had been used as the encroachment angle to establish the criteria of Figure 3, less guardrail protection would have been required.

III. LOCATING GUARDRAIL ON AN EMBANKMENT

Highways that traverse irregular terrain often have sections where considerable fill heights are required. Right-of-way necessary to obtain relatively flat side slopes in these areas is not always economically feasible. In many cases, guardrail protection is required. Questions that arise are: What combination of embankment slopes should be provided? To what lateral dimension off the shoulder should the embankments extend? Where should the guardrail be placed with respect to the shoulder's edge?

A typical fill consists of a 6:1 embankment for a distance of 20 feet from the shoulder's edge and then a 1.5:1 embankment to the bottom of the fill. This study was aimed at developing data to assist the highway engineer in determining a safe distance for locating the guardrail from the shoulder's edge, if it is placed on the 6:1 slope.

Approach

Criteria for the lateral placement of guardrail were obtained by use of HVOSM. The model simulation provided the translational and rotational positions of an automobile as it traversed the roadway shoulder and the 6:1 embankment at selected speeds and angles of encroachment. With the orientation known, the position of the automobile relative to the guardrail could be determined for any distance from the edge of the shoulder. The expected response of the automobile colliding with the guardrail was then made as a function of the lateral placement of the guardrail.

Figure 6 shows an elevation view and Figure 7 shows a plan view of the roadway embankment. Length L is the distance in question.

The procedure followed was to place the automobile on the roadway, orient it at an angle θ , give it a forward speed, and either permit the automobile to be free wheeling (no steer) or steer it in a manner similar to what a driver may be expected to do. In those cases where the automobile was steered, the actual path of the vehicle was highly dependent on the tire-terrain friction coefficient. For this reason, the response of the steered vehicle was computed for different tire-terrain friction coefficients.

The four computer simulation runs made in this study are shown in Table 7. It was assumed that run 1 represents the most severe encroachment conditions that an out-of-control automobile could attain travelling at 60 mph. Simulation results indicate that the influence of the tire-terrain friction coefficient on the path of the automobile in run 1 was negligible. Runs 2 through 4 were made to determine the ability of a driver to steer back to the roadway and the response of the automobile on pavement surfaces ranging from very slick to practically skid resistant. The 15-degree departure angle approximates the greatest angle at which vehicle control could be maintained for a speed of 60 mph, irregardless of the surface friction conditions. The 875-foot radius approximates the smallest radius at which control could be maintained for the selected speed and roadway embankment.

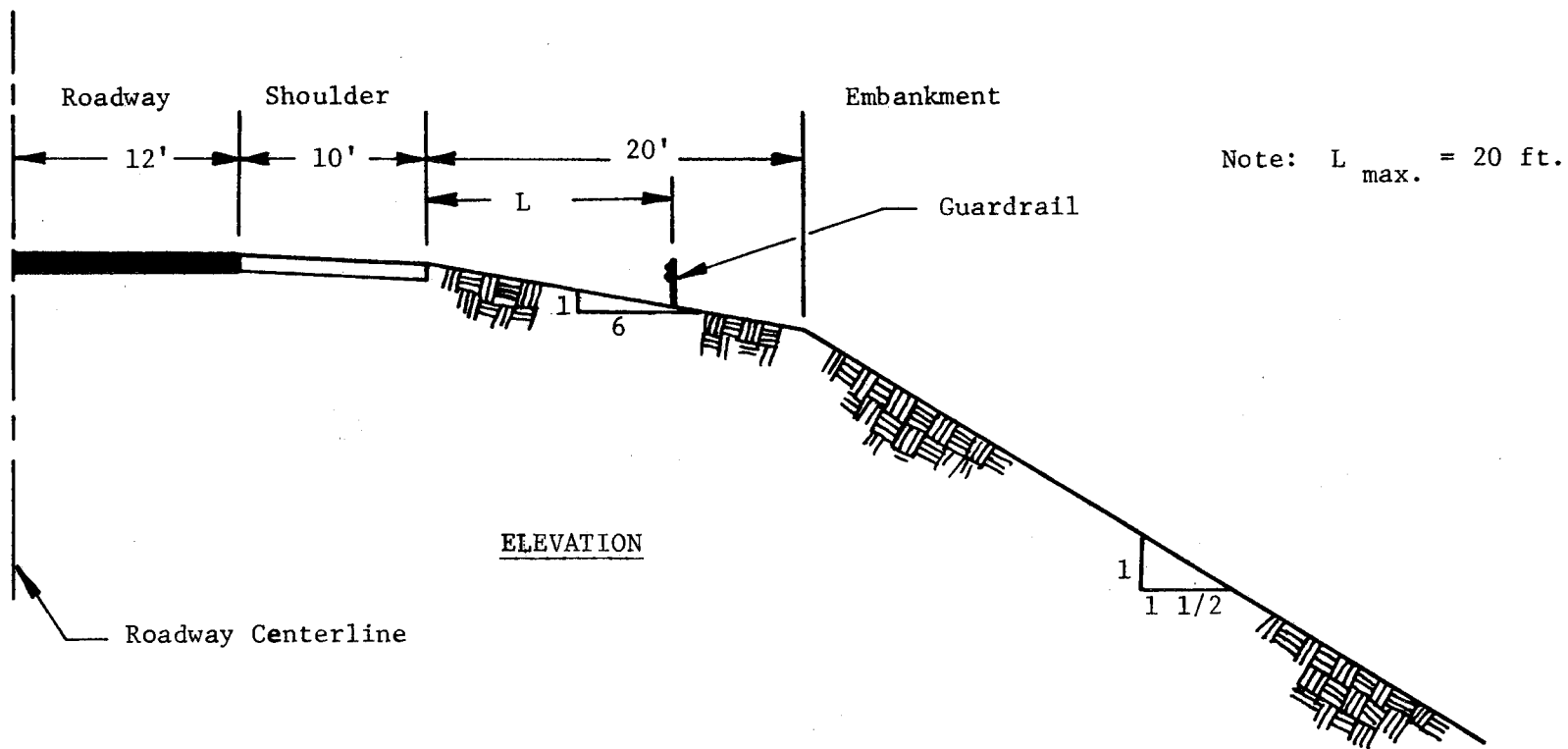


FIGURE 6. ROADSIDE GEOMETRY, ELEVATION VIEW

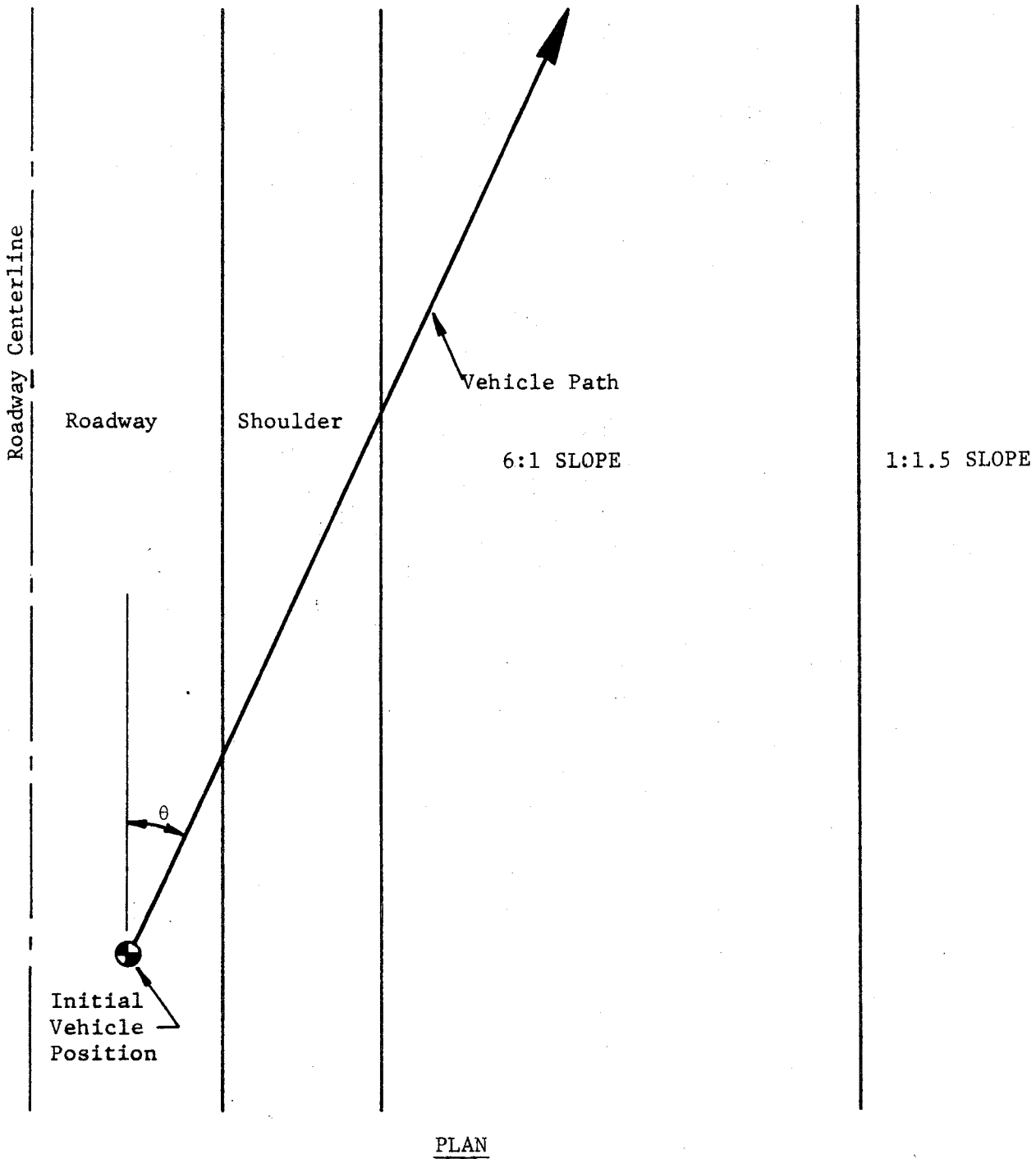


FIGURE 7. ROADSIDE GEOMETRY, PLAN VIEW

TABLE 7. DETAILS OF COMPUTER RUNS

Run No.	Vehicle Velocity (mph)	Encroachment Angle (degree)	Coefficient of Friction	Comments*
1	60	25	0.80	Free wheeling
2	60	15	0.20	Attempted steer back on 875 ft radius
3	60	15	0.6	Attempted steer back on 875 ft radius
4	60	15	1.0	Attempted steer back on 875 ft radius

*In all runs it was assumed that the 6:1 slope extended indefinitely off the shoulder.

Results

In the free-wheeling run the automobile continued essentially along a straight path, deviating very little from the initial 25 degree heading. It remained stable over the embankment width of 20 feet, rolling a maximum of 11.6 degrees and pitching down only 6.2 degrees. The maximum vertical acceleration occurring during the event was 1.1 G's.

Figure 8 shows the paths of the automobile for runs where steer back was attempted. In run 2 ($\mu = 0.2$), very little redirection occurred but the automobile remained stable in the sense that it was never in danger of rolling over. The automobile began a skid after leaving the roadway; and at 20 feet off the shoulder, its heading had changed from 15 degrees to 7.5 degrees (at a zero degree heading it would be parallel to roadway). It rolled a maximum of 13 degrees and pitched down 2.3 degrees. The maximum vertical acceleration occurring during the event was 0.4 G's.

In runs 3 and 4 ($\mu = 0.6$ and $\mu = 1.0$), the automobile remained stable and was successfully redirected back toward the roadway. In both runs the roll angle did not exceed 14.5 degrees and the pitch angle did not exceed 2.0 degrees. The maximum vertical acceleration occurring during the events was 0.5 G's. The results indicate that an automobile leaving the roadway at 15 degrees and 60 mph could probably be steered back to the roadway if the tire-surface friction coefficient was 0.6 or greater and the 6:1 slope extended at least 20 feet from the edge of the shoulder. Some contact would likely occur if the guardrail were 20 feet off the shoulder, but the angle of impact

V = 60 mph
 $\theta = 15^\circ$

LEGEND: \odot Run 2 $\mu = .2$
 \square Run 3 $\mu = .6$
 \triangle Run 4 $\mu = 1.0$

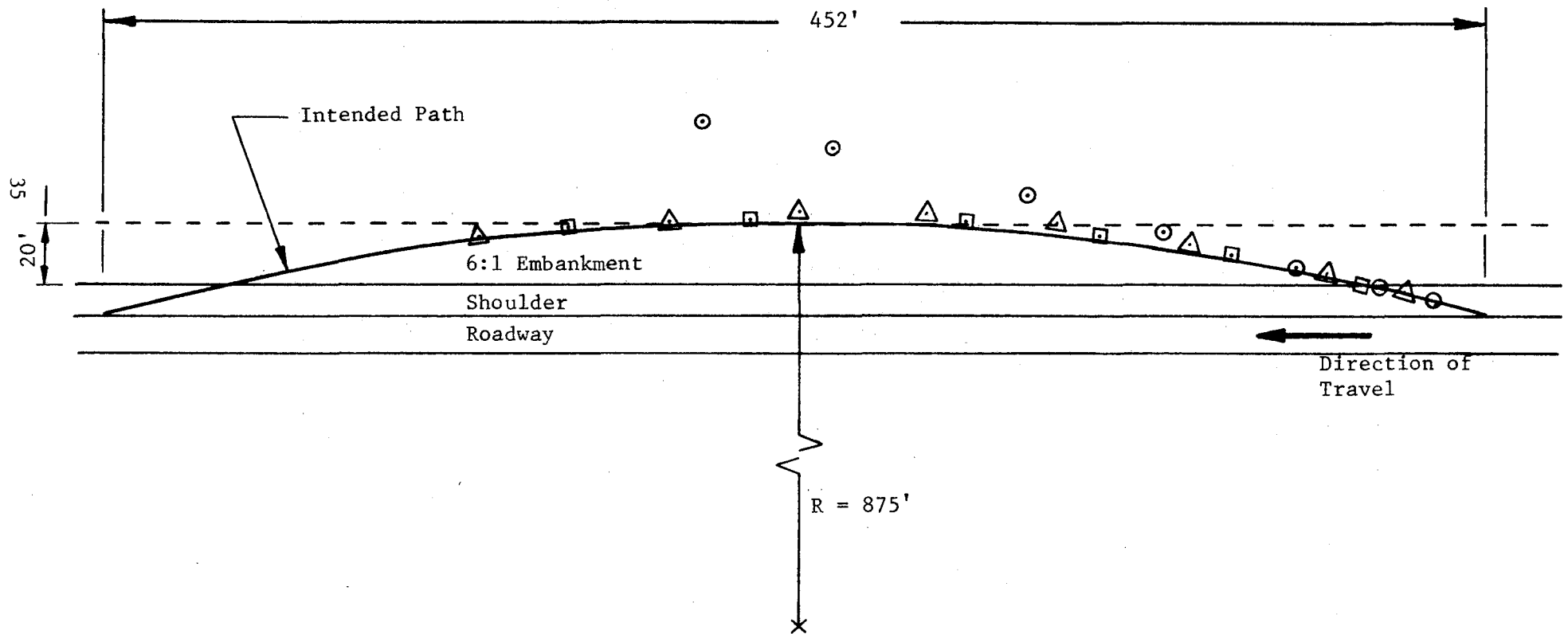


FIGURE 8. VEHICLE PATHS

would be small and the resulting collision forces would probably be small. Tests at low speeds have shown that the lateral coefficient of friction for tires on wet or dry sod exceeds 1.0 on the average (17).

For roadside encroachments (in contrast to median encroachments), the right front bumper is usually the initial point of contact of an automobile in collision with a guardrail. Figures 9 through 12 show the height of the lower and upper parts of the right front bumper above the terrain for the four runs studied. This height may be compared with that of a typical Texas guardrail, which is shown drawn to scale at the right of each figure.

From Figures 9 through 12, it can be seen that guardrail should be located a distance of at least 12 feet from the edge of the shoulder on the 6:1 slope. Between the edge of the shoulder and a distance of 12 feet, the automobile bumper rises above its normal height as much as 5-3/4 inches as shown in Figure 9. Contact with the guardrail in this region would likely cause an automobile with a sloped-back bumper to ramp and possibly vault over the guardrail. The phenomenon of vaulting caused by a sloped-back bumper was discussed by Beaton (10). A distance beyond 12 feet, however, minimizes the chance of vaulting because the height of the bumper becomes lower than its normal height. Also, increasing the distance of the guardrail location provides more recovery area for the driver to steer back to the roadway.

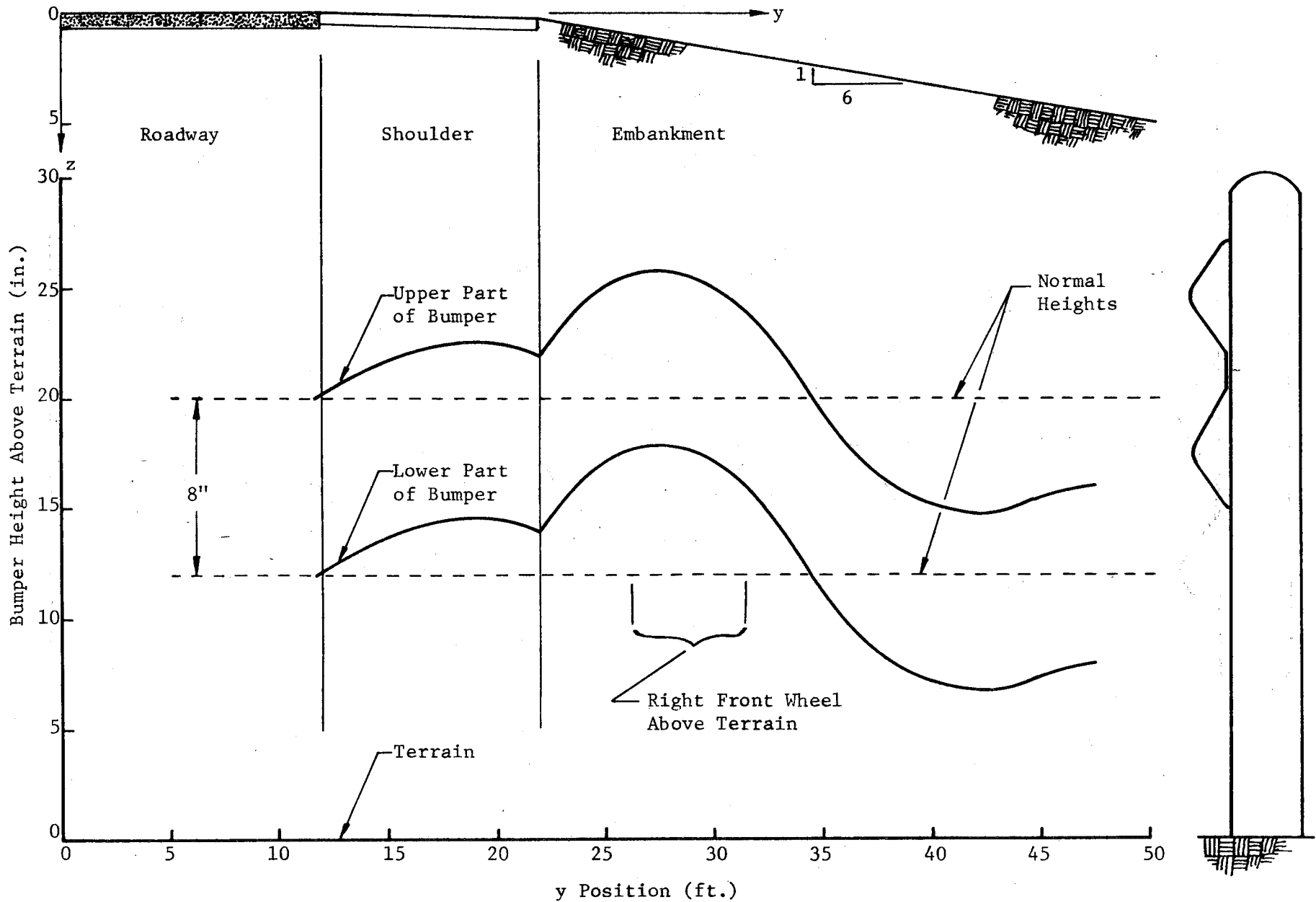


FIGURE 9. RIGHT FRONT BUMPER HEIGHT, RUN 1, 60 MPH, 25°

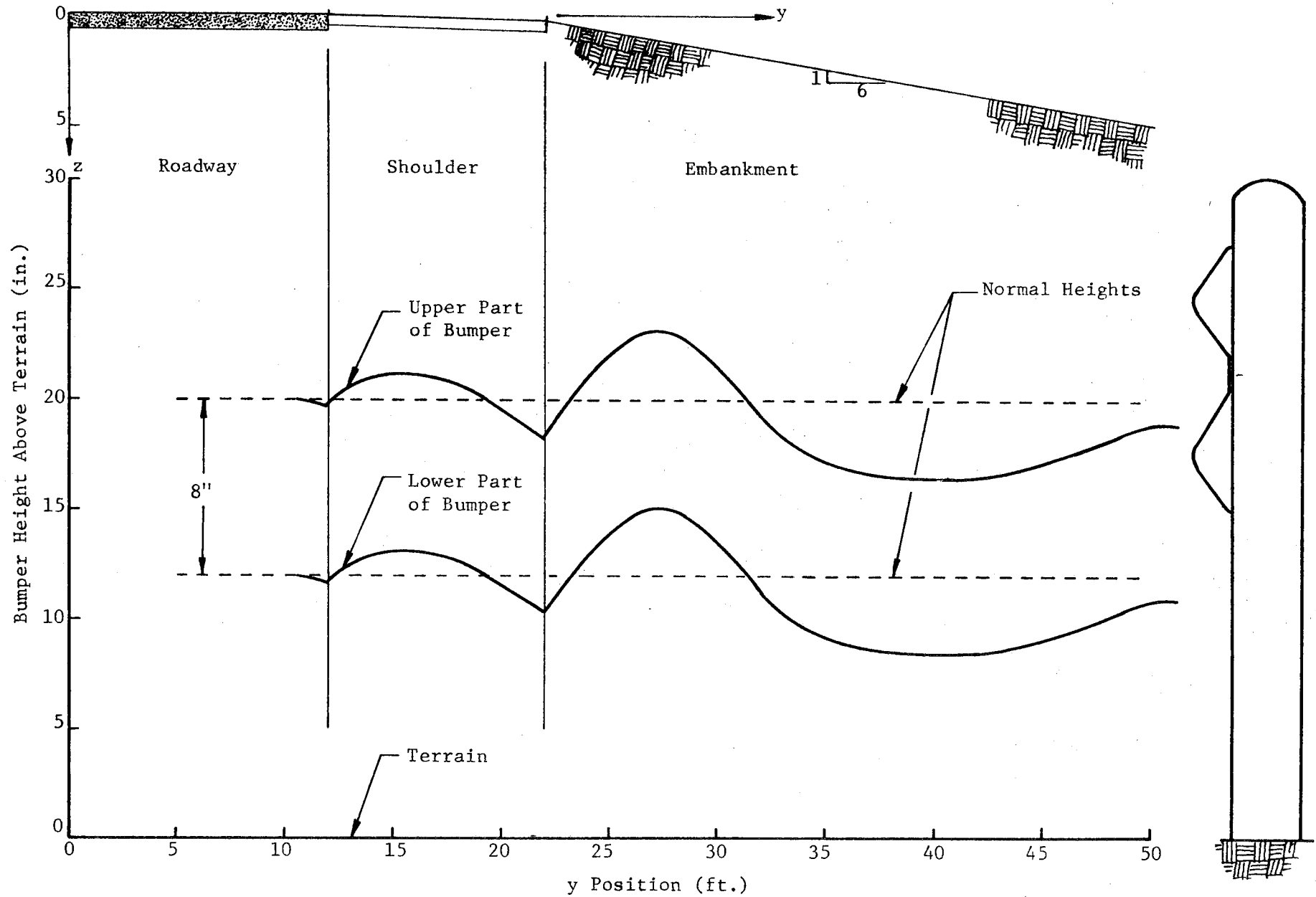


FIGURE 10. RIGHT FRONT BUMPER HEIGHT, RUN 2, 60 MPH, 15°

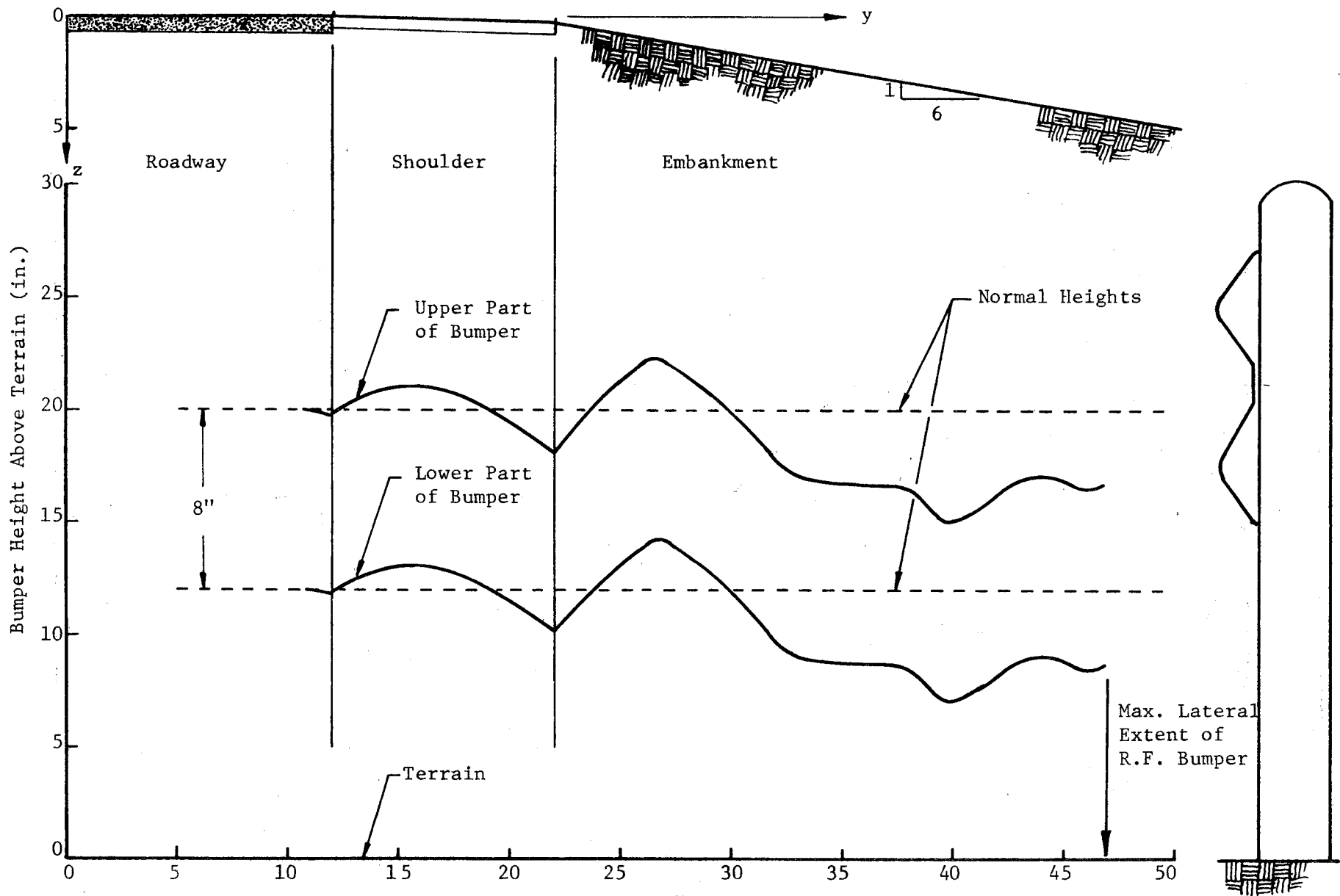


FIGURE 11. RIGHT FRONT BUMPER HEIGHT, RUN 3, 60 MPH, 15°

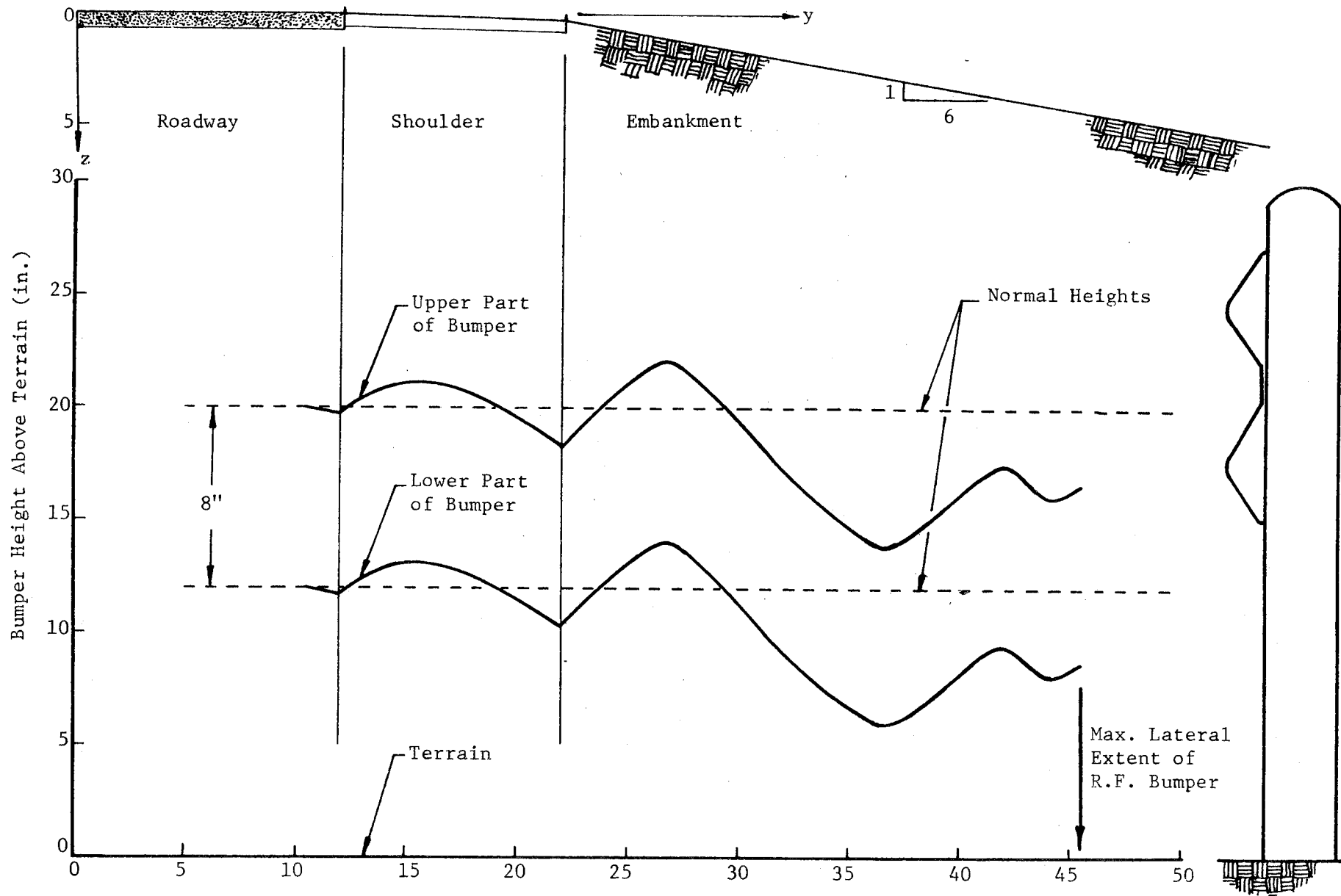


FIGURE 12. RIGHT FRONT BUMPER HEIGHT, RUN 4, 60 MPH, 15°

IV. CONCLUSIONS

1. Criteria are presented for making objective decisions on the need for guardrail protection for embankments. The guardrail system for which these criteria are applicable is the steel W-beam supported on post spaced at 6 ft-3 in. centers. The criteria, which are presented on one graph for conciseness and ease of application, show that sideslopes flatter than 3:1 do not require protection, regardless of the fill height. If adopted, the criteria could result in considerably less of this type of guardrail for embankment protection than is now required by present criteria.
2. The criteria referred to in item 1 were based on an automobile encroachment condition of 25-degree departure angle and 60 mph speed. If the roadway conditions (width, skid number, etc.) are such that the 25-degree departure angle is not attainable, different need criteria would have to be developed for lower encroachment angles.
3. The analysis techniques used in this study, consisting of both math models and full-scale tests, could be used to develop need criteria for various types of guardrail and for various encroachment conditions.
4. If guardrail is placed off the shoulder on a 6:1 sideslope it should be placed 12 feet or more from the shoulder's edge. In so doing, the probability of an automobile ramping and vaulting over the rail will be minimized.

ACKNOWLEDGEMENTS

The consultation and suggestions of Mr. John Nixon and Mr. Dave Hustace of the Texas Highway Department and Mr. Edward Kristaponis of the Federal Highway Administration during the course of this study were appreciated. The assistance Dr. T. J. Hirsch of TTI provided was also appreciated.

REFERENCES

1. McHenry, R. R., and Segal, D. J., "Determination of Physical Criteria for Roadside Energy Conversion Systems," Cornell Aeronautical Laboratory Report No. VJ-2251-V-1, July 1967.
2. McHenry, R. R., and Deleys, N. J., "Vehicle Dynamics in Single Vehicle Accidents: Validation and Extension of a Computer Simulation," Cornell Aeronautical Laboratory Report No. FJ-2251-V-3, December 1968.
3. Young, R. D., Edwards, T. C., Bridwell, R. J., and Ross, H. E., "Documentation of Input for Single Vehicle Accident Computer Program," Research Report 140-1, Texas Transportation Institute, Texas A&M University, July 1969.
4. Hyde, A. S., "Biodynamics and the Crashworthiness of Vehicle Structures," Wyle Laboratories - Research Staff, Huntsville Facility, Report WR 68-3, Vol. III of V, March 1968.
5. Weaver, G. D., "The Relation of Side Slope Design to Highway Safety," NCHRP Project 20-7, Texas Transportation Institute, Texas A&M University, Report 626-1, February 1970, p. 29.
6. Tamanini, F. J., and Viner, M., "Energy Absorbing Roadside Crash Barriers," Civil Engineering, American Society of Civil Engineers, New York, New York, January 1970.
7. Nordlin, E. F., Woodstrom, J. H., and Hackett, R. P., "Dynamic Tests of the California Type 20 Bridge Barrier Rail Series XXIII," California Division of Highways Materials and Research Laboratory, M&R No. 636459, September 1970, pp. A6-7.
8. Michie, J. D., Calcote, L. R., and Bronstad, M. E., "Guardrail Performance and Design," SwRI Project No. 03-2176, NCHRP Final Report No. 15-1 (2), January 1970.
9. Olson, R. M., Post, E. R., and McFarland, "Tentative Service Requirements for Bridge Rail Systems," NCHRP 86, 1970, pp. 11-12.
10. Beaton, J. L., Nordlin, E. F., and Field, R. N., "Dynamic Tests of Corrugated Metal Beam Guardrail," HRR 174, 1967, p. 46.
11. Glennon, J. C., and Tamburri, T. N., "Objective Criteria for Guardrail Installation," HRR 174, 1967, p. 192.

REFERENCES (Continued)

12. Tutt, P. R., and Nixon, J. F., "Roadside Design Guidelines," HRR Special Report 107, 1970, p. 124.
13. Michalski, C. S., "Model Vehicle Damage Scale: A Performance Test," Traffic Safety, Vol. 12, No. 2, June 1968, pp. 34-39.
14. Ross, H. E., Jr., and Post, E. R., "Criteria for the Design of Safe Sloping Culvert Grates," Research Report 140-3, Texas Transportation Institute, Texas A&M University, August, 1971.
15. Young, R. D., "A Three-Dimensional Mathematical Model of an Automobile Passenger," Research Report 140-2, Texas Transportation Institute, Texas A&M University, August, 1970.
16. Committee on Guardrails and Guide Posts, Highway Research Board Circular 482, September, 1962.
17. Stonex, K. A., "Roadside Design for Safety," Presented at 39th Annual Meeting of the Highway Research Board, Washington, D. C., March, 1960.

NOMENCLATURE

- G_{LONG} = automobile acceleration in longitudinal x-axis, G's;
- G_{LAT} = automobile acceleration in lateral y-axis, G's;
- G_{VERT} = automobile acceleration in vertical z-axis, G's;
- G_{XL} = limit acceleration in longitudinal x-axis, G's;
- G_{YL} = limit acceleration in lateral y-axis, G's;
- G_{ZL} = limit acceleration in vertical z-axis, G's;
- G_{LAT}^* = lateral automobile acceleration perpendicular to guardrail centerline, G's;
- G_{LONG}^* = longitudinal automobile acceleration parallel to guardrail centerline, G's;
- V_I = automobile impact speed into guardrail, mph;
- θ = automobile impact angle into guardrail, deg.;
- θ_1 = encroachment angle of automobile leaving roadway, deg.;
- θ_2 = encroachment angle of automobile as it contacts ditch, deg.;
- AL = distance from front of bumper to center-of-mass of automobile, ft.;
- ZB = width of automobile, ft.;
- μ = coefficient-of-friction between automobile and guardrail (assumed as $\mu = 0.3$);
- D = dynamic displacement of guardrail, ft.; and
- g = acceleration due to gravity, 32.2 ft/sec².



APPENDIX A

APPENDIX A

MATHEMATICAL MODEL OF AN AUTOMOBILE

To facilitate in the evaluation and design of a roadway and its environment, it is important to understand what effects that various roadway geometric features have on the dynamic behavior of an automobile and its occupants.

The mathematical model described herein was used to investigate the dynamic behavior of an automobile traversing embankments of various height and slope. In general, the model can be utilized to investigate various problems associated with the roadway environment, such as highway traffic barrier collisions, rapid lane change maneuvers, handling response on horizontal curves, drainage ditch cross sections, and others.

The mathematical model was developed by Cornell Aeronautical Laboratory (CAL) (1, 2) and later modified for specific problem studies by the Texas Transportation Institute (TTI) (3). A conceptual idealization of the model is shown in Figure A1. The model is idealized as four rigid masses, which include: (a) the sprung mass (M_S) of the body supported by the springs, (b) the unsprung masses (M_1 and M_2) of the left and right independent suspension system of the front wheels, and (c) the unsprung mass (M_3) representing the rear axle assembly.

The eleven degrees of freedom of the model include translation of the automobile in three directions measured relative to some fixed coordinate axes system; rotation about the three coordinate of the automobile; independent displacement of each front wheel suspension

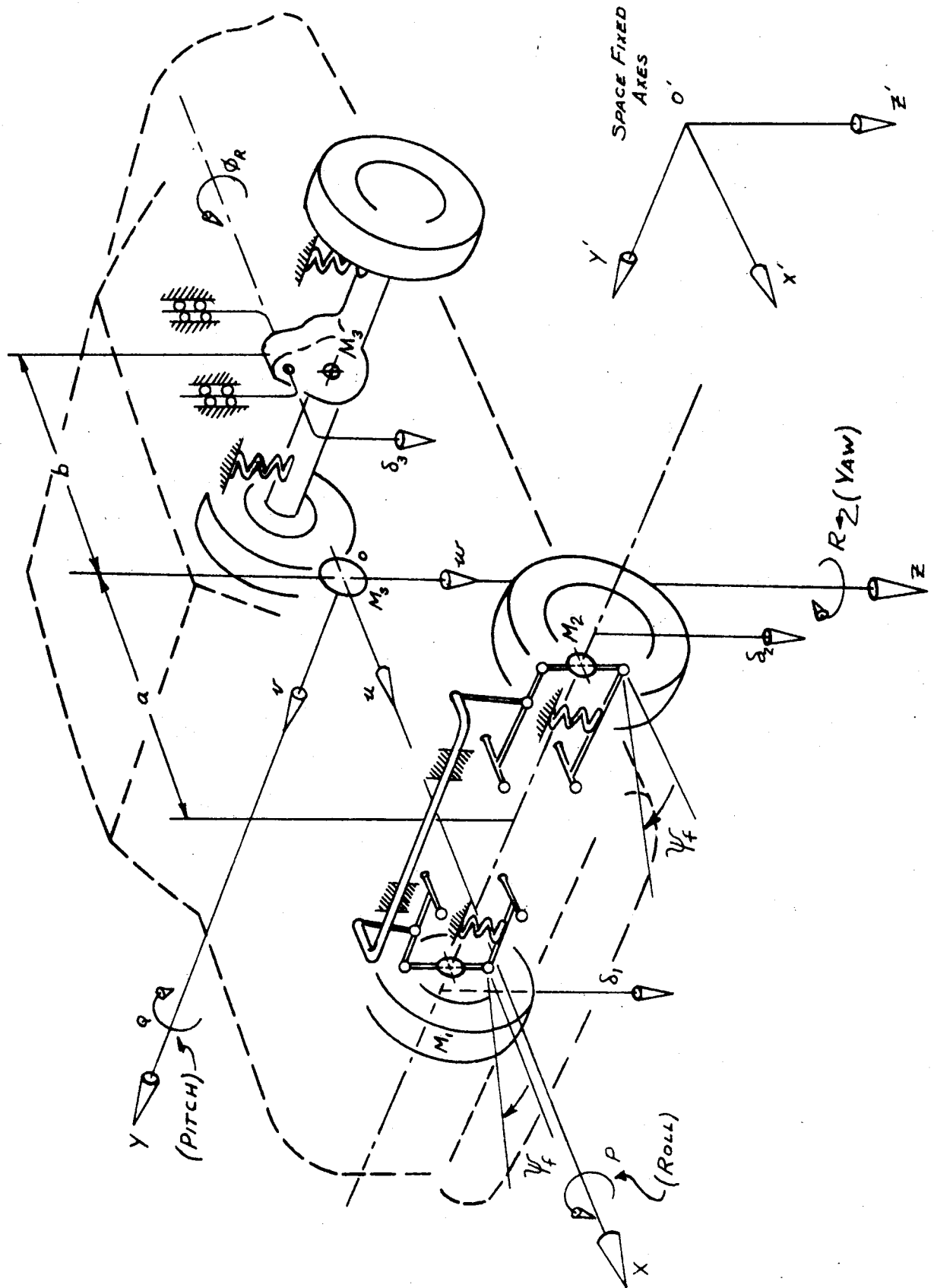


FIGURE A1. IDEALIZATION OF AUTOMOBILE (1,2)

system; suspension displacement and rotation of the rear axle assembly; and steer of the front wheels. If interested, the reader is referred to the references quoted earlier for a more in depth discussion of the mathematical model.

The validity of the model is dependent to a large extent on the accuracy of the input parameters pertaining to the automobile selected. In this study, a 1963 Ford Galaxie, four door sedan was selected because of: (a) the availability of data on the automobile input parameters; (b) the excellent comparisons obtained by CAL (1,2) between full-scale tests and mathematical simulation during a variety of maneuvers; and (c) it is representative of a large population of automobiles from a size and weight standpoint.

Mathematical simulation provides a rapid and economical method to investigate the many parameters involved as an automobile traverses some defined embankment configuration. Once the limiting parameters are identified, it may be desirable to conduct a limited number of full-scale tests prior to final selection of a particular design. This approach, in contrast to a full-scale trial-and-error approach, will yield more meaningful results with considerably less resource expenditure.

APPENDIX B

APPENDIX B

EVALUATION CRITERIA

An acceleration severity-index was used in this study to evaluate the relative hazard of an automobile: (a) being redirected by a 12 Ga. W-Beam guardrail with posts spaced 6 ft.-3 in. on centers, and (b) traversing various height and slope embankments constructed on level terrain.

A discussion of the acceleration severity-index was given in an earlier report (14). For completeness, that discussion is repeated here in more detail. The index takes into consideration the combined effects of the longitudinal, lateral, and vertical accelerations of the automobile at its center-of-mass. A severity-index of unity and less indicates that an unrestrained occupant will not be seriously injured. The equation used to compute the severity-index was similar to an equation presented in a recent publication by Hyde (4) of Wyle Laboratories. The severity-index equation is:

$$SI^* = \sqrt{\left(\frac{G_{LONG.}}{G_{XL}}\right)^2 + \left(\frac{G_{LAT.}}{G_{YL}}\right)^2 + \left(\frac{G_{VERT.}}{G_{ZL}}\right)^2} \quad (B1)$$

The acceleration terms in the numerator of the severity-index equation are the measured or computed values of the automobile; whereas, the acceleration terms in the denominator of the severity-index are the "limit" accelerations of the automobile that an unrestrained occupant can sustain without serious or fatal injury. The development of Equation B1 is presented in Appendix C.

*Mathematical symbols are defined in NOMENCLATURE of this study.

Human body peak acceleration limits for various rise times, time durations, and directions was presented by Hyde (4) as shown in Figure B1. A technique for constructing the trapezoidal acceleration-time diagram shown in Figure B1 from accelerometer recordings of a ninety-fifth percentile point mass representing an occupant was discussed by Hyde. The acceleration limits shown in Figure B1 define the axes of an ellipsoidal envelope as shown in Figure B2. Hyde indicates that the limits of acceleration are not nominal limits for "no injury" but rather are maximum limits beyond which disabling injury or death may be expected. Therefore, the resultant acceleration of the components in the X, Y, and Z directions should not exceed the ellipsoidal envelope shown in Figure B2 to prevent disabling injury or death. It is to be noted that the "limit" accelerations established by Hyde are those experienced by a human occupant. The research engineers of this study were unable to determine from the report of Hyde what the degree of occupant restraint was on which the limit accelerations shown in Figures B1 and B2 were established.

The relationship between the accelerations experienced by an occupant and the accelerations of an automobile at its center-of-mass is largely dependent on the degree of occupant restraint. In other words, the greater the degree of restraint the more similar are the accelerations experienced by an occupant and the accelerations of an automobile. At the present time, however, accident information shows that in the majority of the accidents occupants are unrestrained. The relationship between accelerations experienced by unrestrained occupants and accelerations of an automobile is continually changing

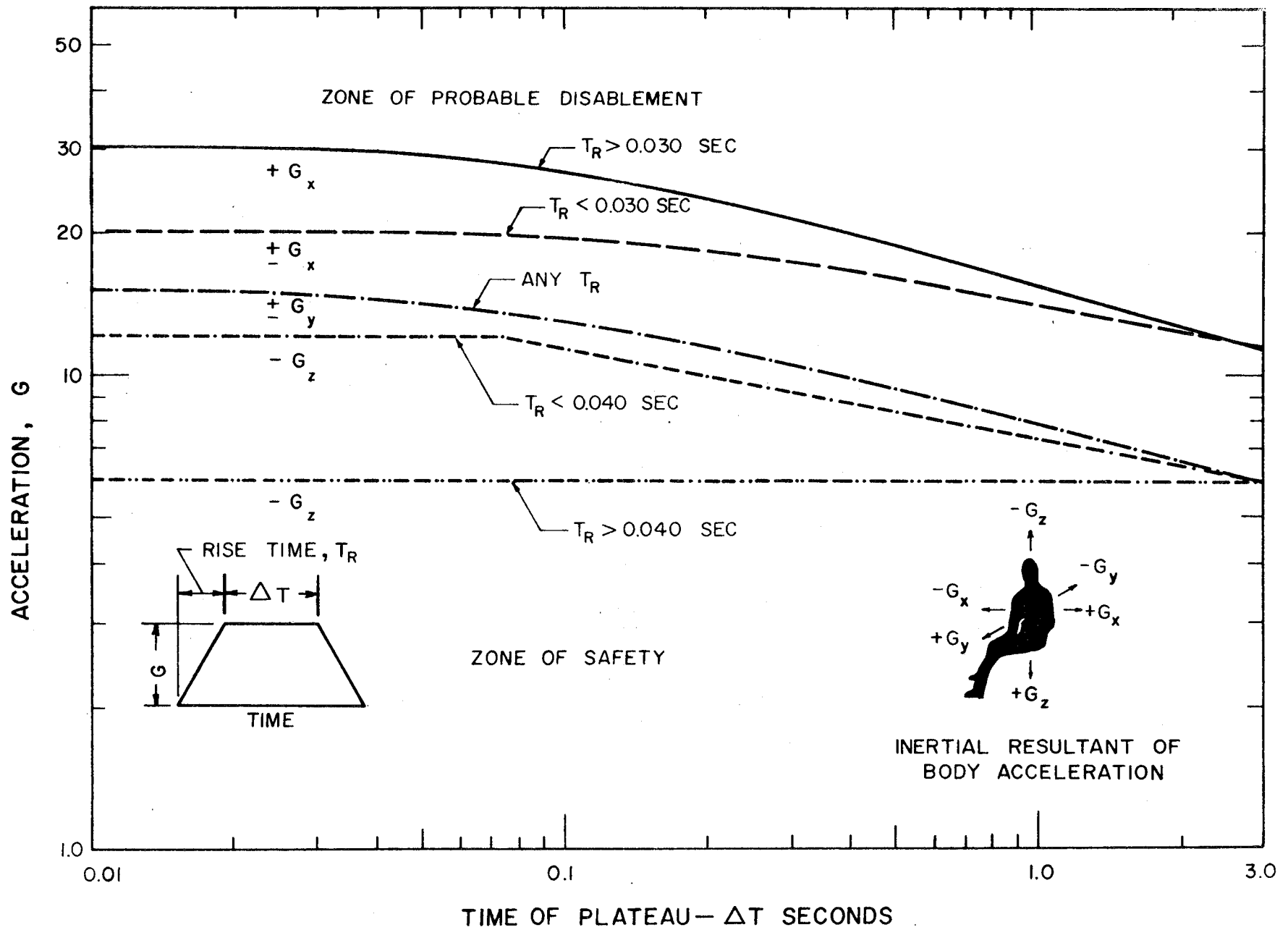
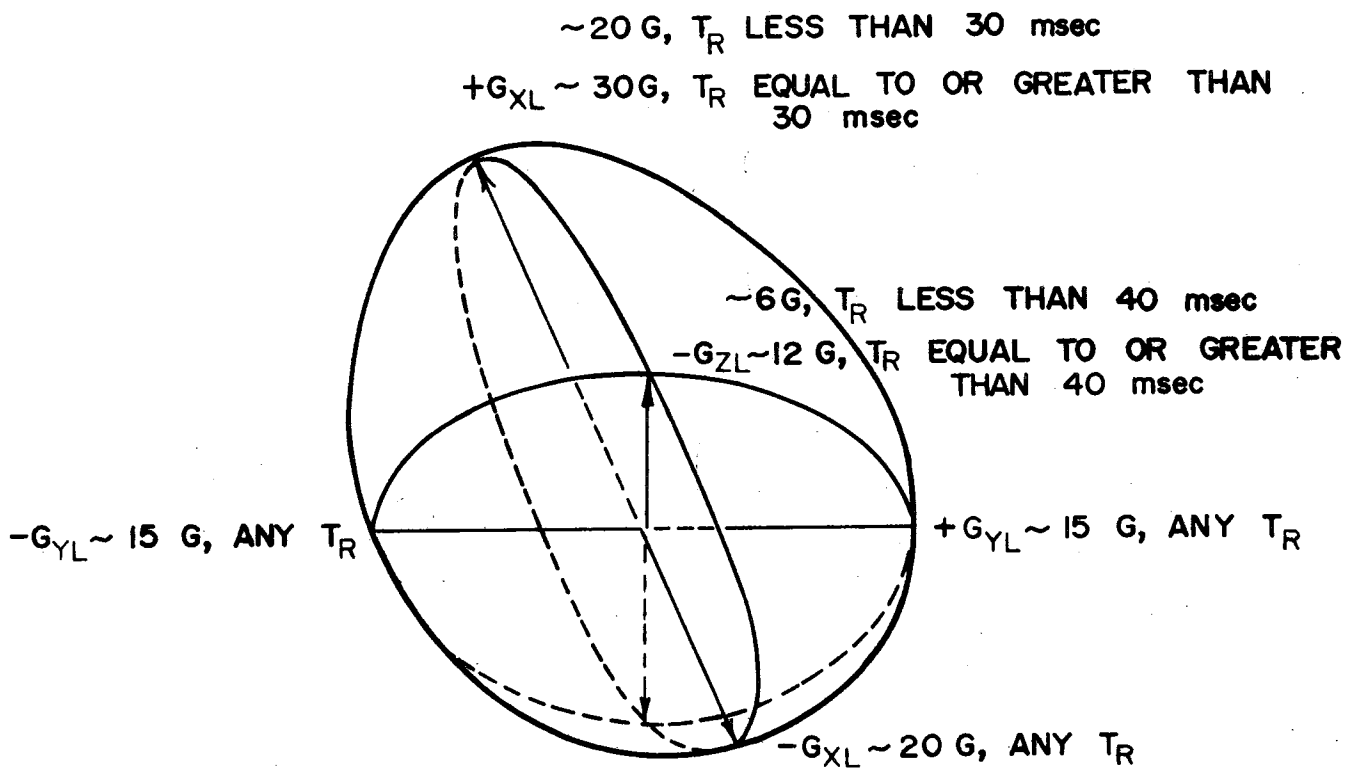
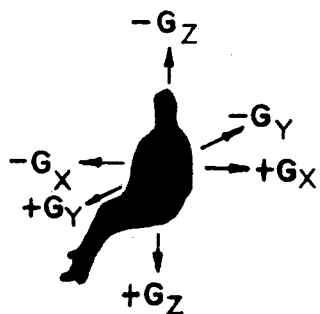


FIGURE B1. HUMAN BODY PEAK ACCELERATION LIMITS FOR VARIOUS RISE TIMES, TIME DURATIONS, AND DIRECTIONS (4)



$+G_{ZL} \sim 17G$, LOW RISK
 $\sim 19.4G$, MEDIUM RISK
 $\sim 22G$, HIGH RISK



INERTIAL RESULTANT OF
 BODY ACCELERATION

FIGURE B2. ELLIPSOIDAL ENVELOPE FOR DEFINING THE MULTIAXIAL ACCELERATION LIMITS(4)

as more and better safety devices are incorporated in automobiles. However, until more sophisticated analysis techniques are developed, the interrelationships between occupant and vehicle will remain largely unknown. Further validation and refinement of an occupant model developed at TTI (15) should help bridge the gap.

Weaver (5) of TTI used the following approach to establish a relationship between human limit accelerations presented by Hyde (4) and automobile accelerations that would be tolerable to an unrestrained occupant. An average automobile deceleration of 12 G's was established in the "4S" program (6) of the Federal Highway Administration as an upper limit for lap belted or lap and shoulder belted occupants during a collision with an energy absorbing roadside crash barrier. Assuming that most accidents involving energy attenuating devices occur head-on or at very shallow impact angles, the 12 G deceleration criteria represents 60 percent of the longitudinal limit acceleration (G_{XL}) established by Hyde (4) for a rise time less than 30 milliseconds. The lateral and vertical automobile accelerations for a lap belt restrained occupant were similarly selected as 60 percent of the values established by Hyde. In turn, Weaver assumed that the limit automobile accelerations for an unrestrained occupant could be taken as 60 percent of the limit automobile accelerations for a lap belt restrained occupant. The limit acceleration limits used in this study were selected in a manner similar to the procedure used by Weaver.

As shown in Figure B1, acceleration limits are a function of both direction and time duration. Two time durations were used in the analysis. On embankments a time duration of 50 milliseconds was

used; whereas, on guardrail collisions time durations of both 50 milliseconds and 225 to 450 milliseconds were used. The limit automobile acceleration values used for these two time durations are shown in Table B1.

It is well known that the accelerations of an automobile may reach very high values over some very small time duration ranging from roughly 2 to 10 milliseconds. Such accelerations are commonly referred to as "spikes". There is much discussion among highway and research engineers as to the significance of "spikes". In a recent publication, Nordlin (7) concluded from an investigation of available literature that the accelerations of an automobile at its center-of-mass should be measured over a time duration of 50 milliseconds. This time duration appears reasonable for automobile embankment traversals because in most of the instances investigated the highest acceleration time duration upon contacting the ditch was less than 80 to 100 milliseconds.

In guardrail impacts, sustained accelerations occur over a longer period of time and it is difficult to select the "appropriate" 50 millisecond period. Since the "limit" accelerations take the duration effects into account, it simplifies the analysis procedure to average the accelerations over the major portion of the event. The longer acceleration time duration used for guardrail collisions was also necessitated by the restrictions imposed by the mathematical model of the vehicle-guardrail collision. It was possible, however, to show that the severity-indices computed from accelerations measured in full-scale crash tests over 50 milliseconds agreed closely with severity-indices computed and measured from accelerations over the longer 225 to 450 millisecond time duration.

TABLE B1

LIMIT ACCELERATIONS (G's)

DIRECTION	HUMAN ACCELERATION LIMITS PRESENTED BY HYDE (4)		LIMIT AUTOMOBILE ACCELERATIONS FOR AN UNRESTRAINED OCCUPANT*	
	50 MS (Figure 2)	275-450 MS (Figure 2)	50 MS	225-450 MS
G_{XL}	20	17	7	6
G_{YL}	15	11	5	4
G_{ZL}	17 (LOW RISK)	Not Needed	6	Not Needed

* Limits selected in a manner similar to the procedure used by Weaver (5).

APPENDIX C

APPENDIX C
SEVERITY-INDEX

The severity-index takes into consideration the combined effects of the automobile acceleration components at its center-of-mass in the longitudinal (X-axis), lateral (Y-axis), and vertical (Z-axis) directions. The severity-index is computed using the following formula:

$$SI^* = \sqrt{\left(\frac{G_{LONG}}{G_{XL}}\right)^2 + \left(\frac{G_{LAT}}{G_{YL}}\right)^2 + \left(\frac{G_{VERT}}{G_{ZL}}\right)^2} \quad (C1)$$

The automobile acceleration components in the numerator are the measured or computed accelerations, whereas, the acceleration components in the denominator are the limit automobile accelerations that would be tolerable for an unrestrained occupant. A severity-index exceeding unity and less indicates that an unrestrained occupant will not be seriously injured.

The limit acceleration components G_{XL} , G_{YL} , and G_{ZL} define the magnitude of the coordinate axes of an ellipsoidal surface as shown in Figure C1. The vector resultant of the limit acceleration components describing an ellipsoidal surface is defined as G_L . It is assumed that the limit acceleration components are symmetrical about the ellipsoidal origin.

* Mathematical symbols are defined in NOMENCLATURE of this study.

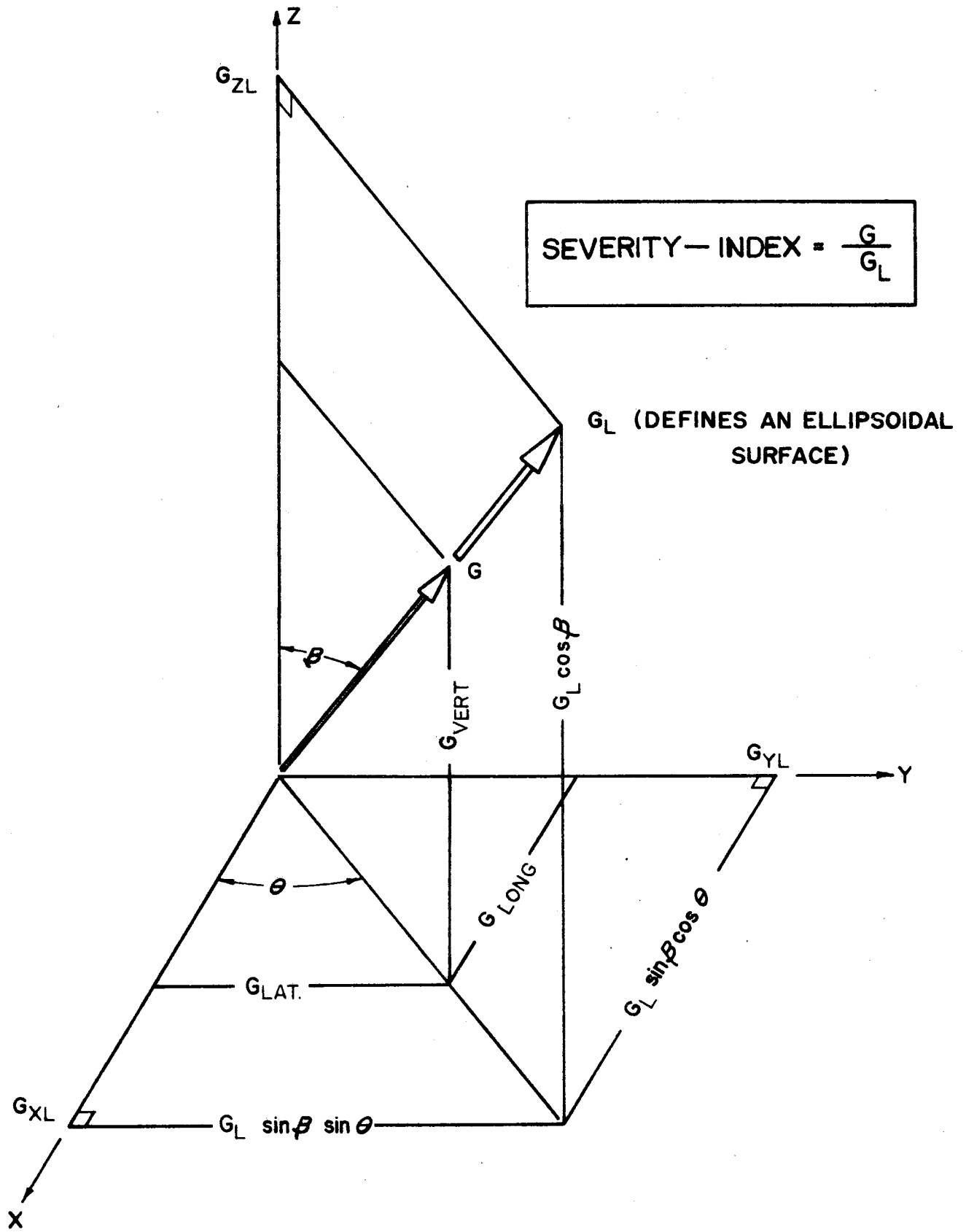


FIGURE CI. MEASURED (OR COMPUTED) AND LIMIT ACCELERATION COMPONENTS

The severity-index is computed as the ratio of the measured or computed resultant automobile acceleration, G , to the resultant limit acceleration, G_L , as follows:

$$\text{Severity-Index, SI} = \frac{G}{G_L} \quad (C2)$$

The general equation of an ellipsoid is:

$$\frac{x^2}{a^2} + \frac{y^2}{b^2} + \frac{z^2}{c^2} = 1 \quad (C3)$$

Referring to Figure C1, it can be seen that:

$$x = G_L \sin\beta \cos\theta \quad (C4)$$

$$y = G_L \sin\beta \sin\theta \quad (C5)$$

$$z = G_L \cos\beta \quad (C6)$$

and, the ellipsoid axes are:

$$a = G_{XL} \quad (C7)$$

$$b = G_{YL} \quad (C8)$$

$$c = G_{ZL} \quad (C9)$$

Substituting Equations C4 through C9 into Equation C3, one obtains:

$$\frac{(G_L \sin\beta \cos\theta)^2}{G_{XL}^2} + \frac{(G_L \sin\beta \sin\theta)^2}{G_{YL}^2} + \frac{(G_L \cos\beta)^2}{G_{ZL}^2} = 1$$

(C10)